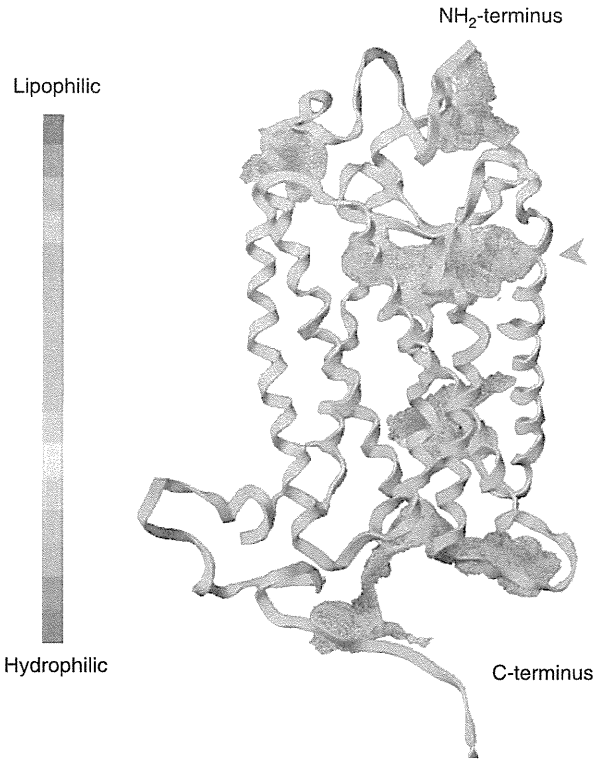

Figure 2. Hydrophobic cavities identified within CCR5. Six hydrophobic cavities are identified within human CCR5, defined using MOLCAD (Sybyl 7.0) [90]. Note the largest hydrophobic cavity (red arrowhead), which is likely to accommodate a molecule of the size of MVC [94], aplaviroc [90], and other CCR5 inhibitors.

Reproduced from [90] with permission of the American Society for Biochemistry and Molecular Biology.

the development of vicriviroc for the treatment of HIV-1 infection was discontinued by Merck in 2010 [69].

5.3 Aplaviroc

Aplaviroc (APL or GSK873140, **Figure 1**), a spirodiketopiperazine derivatives, was developed and reported in 2004 [50]. APL had a high affinity to CCR5 (K_D values of ~3 nM), blocked HIV-1-gp120/CCR5 binding, and exerted potent activity against a wide spectrum of R5-HIV-1 isolates including multi-drug-resistant HIV-1 strains (IC_{50} values of 0.1 – 0.6 nM) *in vitro* [50]. In human peripheral blood mononuclear cell-transplanted R5 HIV-1_{JR-FL}-infected, non-obese diabetic-SCID interleukin-2 receptor γ-chain-knock out mice, in which massive and systemic HIV infection occurred, APL produced ~ 2 $\log_{10}$ reduction in viremia [70]. In Phase IIb clinical trials, patients receiving 600 mg of APL twice daily had a mean decrease in viral load of ~ 1.6 $\log_{10}$ from baseline. The Phase III clinical trials of APL involving ~ 2,000 drug-experienced patients with AIDS were implemented in the United States in the summer of 2005; however, Grade 4 idiosyncratic hepatotoxicity occurred in a few patients and all the trials were terminated [71-73].

5.4 INCB009471

INCB009471, whose structure is related to vicriviroc, exerts potent activity against R5-HIV-1 and exhibits long plasma half-life. Administration of a 200-mg once-daily dose in a 14-day Phase IIa study demonstrated ~ 1.8 $\log_{10}$ reduction in plasma HIV-1 RNA. INCB9471 was safe and well tolerated, and Phase II study was completed, but no further studies are planned at this time [74,75].

5.5 Cenicriviroc

TAK-779, a precursor of cenicriviroc, is the first small-molecule CCR5 inhibitor reported in 1999 [51], which was only moderately active against R5-HIV-1. Optimization of TAK-779 produced TAK-652 (Cenicriviroc or TBR-652, **Figure 1**). Cenicriviroc has good oral bioavailability and long plasma half-life, being expected to allow once-daily administration. In Phase IIa study, cenicriviroc demonstrated potent antiviral activity in treatment-experienced HIV patients. Cenicriviroc also interacts with CCR2, which is known to be associated with inflammation-related diseases, and it is expected to be a potential inflammation mediator as well. In 2011, a Phase IIb clinical trial, in which 150 patients were enrolled, was started to investigate its antiviral, immunologic and anti-inflammatory effects in HIV-1-infected patients [52,76,77].

6. Potential development issues

6.1 Resistance to CCR5 inhibitors

In vitro and *in vivo* studies have suggested the two possible mechanisms, by which CCR5 inhibitors acquire resistance: i) tropism change (X4-HIV-1 becomes predominant in the patient body), or ii) emerging R5-HIV-1 variants that can utilize "drug-bound" CCR5 for viral entry to the cell. *In vitro*, MVC-resistant virus was selected and one isolate had A316T and I323V mutations in the V3 loop of gp120. In the virus assay, such a resistant strain had a unique profile; it showed a decrease in the maximal inhibition with MVC, but its IC_{50} value did not shift substantially [78]. It is considered that this pattern was observed because of the noncompetitive profile of MVC inhibition with gp120 binding to CCR5, and the resistant virus acquired the ability to bind CCR5-drug complex (drug-bound CCR5) [78,79]. MVC-resistant recombinants retained sensitivity to both aplaviroc and enfuvirtide [78]. On the contrary, aplaviroc-resistant virus showed a rightward shift in the IC_{50} and the maximal inhibition level did not change. Mutations related to the aplaviroc sensitivity were shown not only in the V3 region but in the V1 and conserved regions in gp120 [80]. In multiple *in vitro* studies, CCR5-inhibitor-resistant viruses retained the same CCR5 tropism and no occurrence of X4 virus was observed, possibly because of its experimental circumstance (for example, cell lines suitable for R5-HIV-1 replication was used) [81,82]. Westby *et al.* reported that selection of an MVC-resistant R5-HIV-1 (SF162-derived) produced a tropism shift to X4-phenotype; however, this was observed in both MVC and control

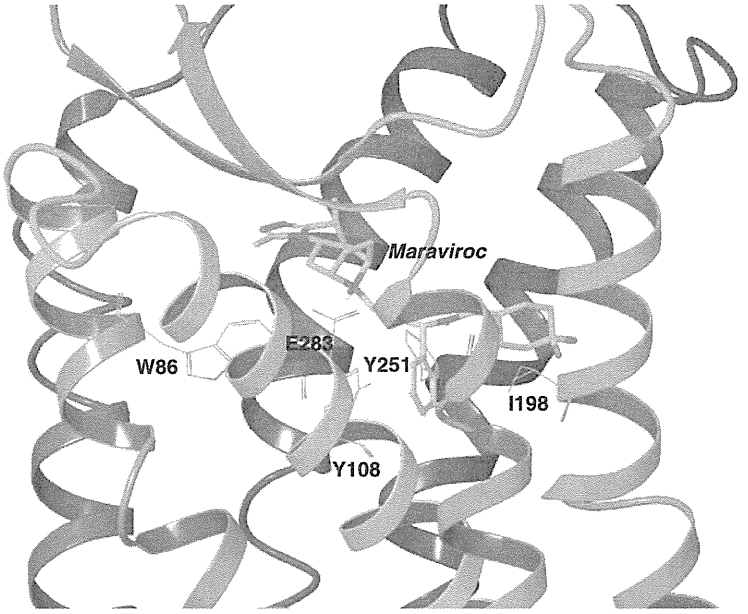

Figure 3. A docked structure of MVC within CCR5. A model of the binding mode of MVC (stick representation) illustrates the relative location of MVC within CCR5. Polar hydrogens are only shown. Note that MVC binds to the hydrophobic cavity shown by a red arrowhead in **Figure 2**, as does aplaviroc [90]. Site-directed mutagenesis experiments conducted by Garcia-Perez *et al.* [94] indicate that MVC has polar interactions with E283 residue, critical for the binding of MVC to CCR5. Other residues important for the binding of MVC are shown in wires.

(no drug) passage cultures, indicating that its appearance was not a result of selective pressure by MVC [78].

A clinical trial (MERIT study) showed that the level of MVC resistance is low if ever, and the virological failure observed was mainly caused by the emergence of X4-HIV-1 that preexisted in patients but was not detected by the tropism assay [83,84]. Other studies (MOTIVATE 1 and 2) showed that 60% patients, who failed treatment with MVC, had X4-HIV-1, while only 6% of patients in the control had X4-HIV-1 [60], indicating that most cases who experienced virological failure with MVC were related to the R5 to X4 tropism change.

6.2 HIV-1 tropism

Prior to initiation of therapy, all patients must take a blood test to determine the tropism (coreceptor usage) of HIV-1 the patient harbors, because CCR5 inhibitors are only active against R5-HIV-1 but not against X4-HIV-1. If some patients have small amounts of X4-HIV-1, even below the detection level, the exposure to a CCR5 inhibitor may allow outgrowth of the X4-HIV-1. The Trofile assay is used to determine the tropism of HIV-1 in patients. In the assay, the virus genome from the patient's HIV-1 is isolated and cloned, the infectious virus is produced, subsequently virus susceptibility to the CCR5 inhibitor is determined using CCR5 and CXCR4 expressing cell lines. In this assay, viral loads >1,000 copies/ml are needed to obtain reliable results, and using the Trofile® enhanced sensitivity assay, 0.3% CXCR4-using HIV-1 variants can be detected with 100% sensitivity [42,58,85]. The requirement of HIV-1 tropism testing before initiation of MVC treatment has been an obstacle for the widened use of MVC. Another way to determine HIV-1 tropism is by genotypic assay [45], which has been favored in European countries over the Trofile® enhanced sensitivity assay. This issue has been described in the "Market review" section of this article.

6.3 Immunological reconstitution

The administration of MVC results in an increase of $CD4^+$ T-cell counts in the blood, a possible advantage that may contribute to an increased immunological function. Of note, this effect was observed in both drug experienced and drug-naïve patients in clinical trials (MOTIVATE 1 & 2, and MERIT study), and even in the group who do not respond virologically to MVC (mean increases of 59 and 43 cells/mm^3 with MVC administration compared with 10 cells/mm^3 in patients treated with placebo; MOTIVATE 1 & 2 studies) [56,63,86]. Recently, Cuzin *et al.* reported a study to address the ability of a 24-week maraviroc intensification of stable and efficient HAART to increase the CD4 cell count slope. In this study, the median slope prior to intensification was +14 cells/µl/year and the slope increased to +23 cells/µl/year in patients who received 24-week maraviroc intensification [87].

6.4 Modeling analysis

While a crystal structure of CCR5 is currently not available, CCR5 structure models have been constructed by homology

modeling technique based on bovine rhodopsin crystal structure [88-90]. **Figure 2** illustrates the three-dimensional model of CCR5 that has a seven transmembrane helical structure. Six hydrophobic cavities were identified in the extracellular, transmembrane, and intracellular domains of CCR5. Among them, a hydrophobic cavity, to which CCR5 inhibitors highly likely bind, was identified (**Figure 2**, red arrow) [90]. In certain studies including ours [90,91], molecular interactions between CCR5 and small-molecule inhibitors were characterized, in which the computational modeling technique was combined with biological data including ligand binding assay using CCR5 mutants [90,91]. Several groups have reported binding modes for CCR5 inhibitors including MVC and aplaviroc. In those studies, all the CCR5 inhibitors have been shown to bind to the same hydrophobic cavity (**Figure 3**) [88-95]. Such approaches of combining site-directed mutagenesis-based data and molecular modeling should be useful for gaining structural insights for developing novel drug design.

7. Conclusion

As of this writing, MVC, a small-molecule CCR5 inhibitor, and enfuvirtide, an oligopeptide fusion inhibitor, are only drugs that have been approved for clinical use as entry inhibitors. Currently, there are only a few entry inhibitors in clinical/preclinical trials. Development of entry inhibitors will undoubtedly improve our ability to manage HIV-1 infection. In particular, development of potent and metabolically-stable novel CCR5 inhibitors with the possibility of once-daily (QD) dosing regimens is urgently needed. Development of CXCR4 inhibitors should complement the limitation of CCR5 inhibitors (i.e., the lack of activity to X4-HIV-1) and greatly improve the efficacy of CCR5 inhibitor-containing regimens.

8. Expert opinion

While the proof-of-principle has been established for the use of entry inhibitors including CCR5 inhibitors for treating HIV-1 infection and AIDS, further data of long-term efficacy of CCR5 inhibitors must be accumulated and examined. Although clinical trials have shown no clinically relevant differences in safety between individuals receiving MVC and those receiving the placebo, the long-term safety of blocking CCR5, a receptor whose function in healthy individuals is not fully understood, is to be determined. Considering the fact that CCR5 inhibitors are active only against R5-HIV-1 strains, there still exist several concerns upon the use of CCR5 inhibitors: i) virtually all HIV-1-infected individuals carry both R5-HIV-1 and X4-HIV-1 and/or dual-tropic HIV-1 species; ii) X4-HIV-1 is known to become predominant when HIV-1 diseases progress; and iii) long-term treatment with CCR5 inhibitors may accelerate the emergence/predominance of X4-HIV-1 and CCR5 inhibitor treatment becomes meaningless. Although the DHHS guideline [42] recommends MVC-containing regimens for treatment-naïve patients, the use of MVC has not been widened. MVC appears to have been used as one of drugs for salvage therapy in heavily ART-experienced patients rather than in drug-naïve patients. This is apparently due to its substantial disadvantages such as its twice-daily dosing schedule in addition to the concerns described above. Another significant disadvantage is that an HIV-1 tropism test such as the costly and time-consuming Trofile enhanced sensitivity assay must be performed prior to the initiation of MVC treatment, an inconvenience for both physicians and patients. The access to inexpensive, highly sensitive, and rapid HIV-1 tropism tests should be made available worldwide. As of this writing, only a few novel CCR5 inhibitors are on the pipeline. Development of more potent and more metabolically-stable novel CCR5 inhibitors with the possibility of once-daily (QD) dosing regimens is urgently needed.

Compared to CCR5 inhibitors, much fewer numbers of CXCR4 inhibitors have been reported as potential therapeutics for treating HIV-1 infection. In fact, no CXCR4 inhibitors have been approved for clinical use as of today. Hence, there is an urgent need for novel small-molecule inhibitors targeting CXCR4. Such CXCR4 inhibitors, if they become clinically available, should greatly improve the treatment options available to patients infected with X4- and/or dual-tropic HIV-1 strains in combination with a CCR5 inhibitor. In this regard, the crystal structures of CXCR4 in complex with CXCR4 inhibitors have recently been solved [96] and opened up the possibility of identifying and designing novel CXCR4 inhibitors.

Acknowledgements

We are thankful to E Kellenberger for providing the coordinates of a model of CCR5-maraviroc complex.

Declaration of interest

The authors of this article have no conflict of interest with entry inhibitors including CCR5 inhibitors that are now in clinical use or in clinical/preclinical development. This work was supported in part by the Intramural Research Program of the Center for Cancer Research, National Cancer Institute, NIH, and in part by a Grant for global education and research center aiming at the control of AIDS (Global Center of Excellence supported by Monbu-Kagakusho), Promotion of AIDS Research from the Ministry of Health, Welfare, and Labor of Japan.

Bibliography

Papers of special note have been highlighted as either of interest (•) or of considerable interest (••) to readers.

1. Mitsuya H, Weinhold KJ, Furman PA, et al. 3'-Azido-3'-deoxythymidine (BW A509U): an antiviral agent that inhibits the infectivity and cytopathic effect of human T-lymphotropic virus type III/ lymphadenopathy-associated virus in vitro. Proc Natl Acad Sci USA 1985;82:7096-100
2. Mitsuya H, Erickson J. Discovery and development of antiretroviral therapeutics for HIV infection. In: Merigan TC, Bartlet JG, Bolognesi D, editors. Textbook of AIDS Medicine. Williams & Wilkins; Baltimore: 1999. p. 751-80
3. Murphy EL, Collier AC, Kalish LA, et al. Highly active antiretroviral therapy decreases mortality and morbidity in patients with advanced HIV disease. Ann Intern Med 2001;135:17-26
4. Hogg R, Lima V, Sterne JA, et al. Life expectancy of individuals on combination antiretroviral therapy in high-income countries: a collaborative analysis of 14 cohort studies. Lancet 2008;372:293-9
5. Bhaskaran K, Hamouda O, Sannes M, et al. Changes in the risk of death after HIV seroconversion compared with mortality in the general population. JAMA 2008;300:51-9
6. Walensky RP, Paltiel AD, Losina E, et al. The survival benefits of AIDS treatment in the United States. J Infect Dis 2006;194:11-19
7. Gupta R, Hill A, Sawyer AW, et al. Emergence of drug resistance in HIV type 1-infected patients after receipt of first-line highly active antiretroviral therapy: a systematic review of clinical trials. Clin Infect Dis 2008;47:712-28
8. Fauci AS. HIV and AIDS: 20 years of science. Nat Med 2003;9:839-43
9. Hirsch HH, Kaufmann G, Sendi P, et al. Immune reconstitution in HIV-infected patients. Clin Infect Dis 2004;38:1159-66
10. Bleul CC, Farzan M, Choe H, et al. The lymphocyte chemoattractant SDF-1 is a ligand for LESTR/fusin and blocks HIV-1 entry. Nature 1996;382:829-33
11. Trkola A, Dragic T, Arthos J, et al. CD4-dependent, antibody- sensitive interactions between HIV-1 and its coreceptor CCR-5. Nature 1996;384:184-7
12. Deng H, Liu R, Ellmeier W, et al. Identification of a major co-receptor for primary isolates of HIV-1. Nature 1996;381:661-6
13. Wu L, Gerard NP, Wyatt R, et al. CD4-induced interaction of primary HIV-1 gp120 glycoproteins with the chemokine receptor CCR-5. Nature 1996;384:179-83
14. Doranz BJ, Rucker J, Yi Y, et al. A dual-tropic primary HIV-1 isolate that uses fusin and the beta- chemokine receptors CKR-5, CKR-3, and CKR-2b as fusion cofactors. Cell 1996;85:1149-58
15. Choe H, Farzan M, Sun Y, et al. The beta- chemokine receptors CCR3 and CCR5 facilitate infection by primary HIV-1 isolates. Cell 1996;85:1135-48
16. Dragic T, Litwin V, Allaway GP, et al. HIV-1 entry into CD4+ cells is mediated by the chemokine receptor CC- CKR-5. Nature 1996;381:667-73
17. Alkhatib G, Combadiere C, Broder CC, et al. CC CKR5: a RANTES, MIP-1alpha, MIP-1beta receptor as a fusion cofactor for macrophage-tropic HIV-1. Science 1996;272:1955-8
18. Feng Y, Broder CC, Kennedy PE, Berger EA. HIV-1 entry cofactor: functional cDNA cloning of a seven-transmembrane, G protein-coupled receptor. Science 1996;272:872-7

•• **First report that the chemokine receptor CXCR4 is an HIV-1 coreceptor.**

19. Rizzuto CD, Wyatt R, Hernandez-Ramos N, et al. A conserved HIV gp120 glycoprotein structure involved in chemokine receptor binding. Science 1998;280:1949-53
20. Poignard P, Saphire EO, Parren PW, Burton DR. Gp120: biologic aspects of structural features. Annu Rev Immunol 2001;19:253-74
21. Kwong PD, Wyatt R, Robinson J, et al. Structure of an HIV gp120 envelope glycoprotein in complex with the CD4 receptor and a neutralizing human antibody. Nature 1998;393:648-59

• **Report of HIV-gp120 crystal structure, authors also suggested structural interaction of gp120 with CD4 and CCR5 which induces HIV entry.**

22. Kilby JM, Eron JJ. Novel therapies based on mechanisms of HIV-1 cell entry. N Engl J Med 2003;348:2228-38
23. Jahn R, Lang T, Sudhof TC. Membrane fusion. Cell 2003;112:519-33
24. Chan DC, Fass D, Berger JM, Kim PS. Core structure of gp41 from the HIV envelope glycoprotein. Cell 1997;89:263-73
25. Chan DC, Kim PS. HIV entry and its inhibition. Cell 1998;93:681-4
26. Littman DR. Chemokine receptors: keys to AIDS pathogenesis? Cell 1998;93:677-80
27. Hoffman TL, Doms RW. Chemokines and coreceptors in HIV/SIV-host interactions. AIDS 1998;12(Suppl A):S17-26
28. Doranz BJ, Berson JF, Rucker J, Doms RW. Chemokine receptors as fusion cofactors for human immunodeficiency virus type 1 (HIV-1). Immunol Res 1997;16:15-28
29. Berger EA. HIV entry and tropism: the chemokine receptor connection. AIDS 1997;11:S3-16
30. Berger EA, Murphy PM, Farber JM. Chemokine receptors as HIV-1 coreceptors: roles in viral entry, tropism, and disease. Annu Rev Immunol 1999;17:657-700
31. Connor RI, Sheridan KE, Ceradini D, et al. Change in coreceptor use coreceptor use correlates with disease progression in HIV-1-infected individuals. J Exp Med 1997;185:621-8
32. de Roda Husman AM, Schuitemaker H. Chemokine receptors and the clinical course of HIV-1 infection. Trends Microbiol 1998;6:244-9
33. O'Brien SJ, Moore JP. The effect of genetic variation in chemokines and their receptors on HIV transmission and progression to AIDS. Immunol Rev 2000;177:99-111
34. Samson M, Libert F, Doranz BJ, et al. Resistance to HIV-1 infection in Caucasian individuals bearing mutant alleles of the CCR-5 chemokine receptor gene. Nature 1996;382:722-5
35. Dean M, Carrington M, Winkler C, et al. Genetic restriction of HIV-1 infection and progression to AIDS by a deletion allele of the CKR5 structural gene. Hemophilia

Growth and Development Study, Multicenter AIDS Cohort Study, Multicenter Hemophilia Cohort Study, San Francisco City Cohort, ALIVE Study. Science 1996;273:1856-62

• **Authors showed CCR5 deletion resulted in the delay of AIDS progression.**

36. Liu R, Paxton WA, Choe S, et al. Homozygous defect in HIV-1 coreceptor accounts for resistance of some multiply-exposed individuals to HIV-1 infection. Cell 1996;86:367-77

37. Glass WG, McDermott DH, Lim JK, et al. CCR5 deficiency increases risk of symptomatic West Nile virus infection. J Exp Med 2006;203:35-40

38. Bracci PM, Skibola CF, Conde L, et al. Chemokine polymorphisms and lymphoma: a pooled analysis. Leuk Lymphoma 2010;51:497-506

39. AIDS epidemic update. World Health Organization. Available from: http://www.unaids.org/en/media/unaids/contentassets/dataimport/pub/report/2009/jc1700 _epi_update_2009_en.pdf [Last accessed 12 December 2011]

40. Global Report: UNAIDS Report on the Global AIDS Epidemic 2010. UNAIDS. Available from: http://www.unaids.org/globalreport/Global_report.htm [Last accessed 12 December 2011]

41. Impact of the Global Financial and Economic Crisis on the AIDS Response. 25th Meeting of the UNAIDS Programme Coordinating Board: UNAIDS, 2009. Available from: http://www.unaids.org/en/ [Last accessed 12 December 2011]

42. Guidelines for the Use of Antiretroviral Agents in HIV-1-Infected Adults and Adolescents. DHHS Panel on Antiretroviral Guidelines for Adults and Adolescents – A Working Group of the Office of AIDS Research Advisory Council (OARAC) (January 10, 2011)

43. Chapman D, Valdez H, Lewis M, et al. Clinical, virologic, and immunologic characteristics of patients with discordant phenotypic and genotypic co-receptor tropism test results. Paper presented at: 50th Interscience Conference on Antimicrobial Agents and Chemotherapy; 12 – 15 September 2010; Boston, MA

44. McGovern RA, Thielen A, Mo T, et al. Population-based V3 genotypic tropism assay: a retrospective analysis using screening samples from the A4001029 and MOTIVATE studies. AIDS 2010;24:2517-25

45. Vandekerckhove LP, Wensing AM, Kaiser R, et al. European Consensus Group on clinical management of tropism testing. European guidelines on the clinical management of HIV-1 tropism testing. Lancet Infect Dis 2011;11:394-407

46. Cocchi F, DeVico AL, Garzino-Demo A, et al. Identification of RANTES, MIP-1 alpha, and MIP-1 beta as the major HIV-suppressive factors produced by CD8+ T cells. Science 1995;270:1811-15

47. Dorr P, Westby M, Dobbs S, et al. Maraviroc (UK-427,857), a potent, orally bioavailable, and selective small-molecule inhibitor of chemokine receptor CCR5 with broad-spectrum antihuman immunodeficiency virus type 1 activity. Antimicrob Agents Chemother 2005;49:4721-32

48. Strizki JM, Xu S, Wagner NE, et al. SCH-C (SCH 351125), an orally bioavailable, small molecule antagonist of the chemokine receptor CCR5, is a potent inhibitor of HIV-1 infection in vitro and in vivo. Proc Natl Acad Sci USA 2001;98:12718-23

49. Tagat JR, McCombie SW, Nazareno D, et al. Piperazine-based CCR5 antagonists as HIV-1 inhibitors. IV. Discovery of 1-[(4,6-dimethyl-5-pyrimidinyl)carbonyl]-4-[4-[2-methoxy-1(R)-4-(trifluoromethyl) phenyl]ethyl- 3(S)-methyl-1- piperazinyl]-4-methylpiperidine (Sch-417690/Sch-D), a potent, highly selective, and orally bioavailable CCR5 antagonist. J Med Chem 2004;47:2405-8

50. Maeda K, Nakata H, Koh Y, et al. A spirodiketopiperazine-based CCR5 inhibitor which preserves CC-chemokine/CCR5 interactions and exerts potent activity against R5 HIV-1 in vitro. J Virol 2004;78:8654-62

51. Baba M, Nishimura O, Kanzaki N, et al. A small- molecule, nonpeptide CCR5 antagonist with highly potent and selective anti-HIV-1 activity. Proc Natl Acad Sci USA 1999;96:5698-03

•• **Report on TAK-779, which is the first small molecule CCR5 antagonist.**

52. Seto M, Aikawa K, Miyamoto N, et al. Highly potent and orally active CCR5 antagonists as anti-HIV-1 agents: synthesis and biological activities of 1-benzazocine derivatives containing a sulfoxide moiety. J Med Chem 2006;49:2037-48

53. Parra J, Portilla J, Pulido F, et al. Clinical utility of maraviroc. Clin Drug Investig 2011;31:527-42

54. Daniel R, Kuritzkes MD. HIV-1 Entry Inhibitors: an Overview. Curr Opin HIV AIDS 2009;4:82-7

55. Fatkenheuer G, Pozniak AL, Johnson MA, et al. Efficacy of short-term monotherapy with maraviroc, a new CCR5 antagonist, in patients infected with HIV-1. Nat Med 2005;11:1170-2

•• **Report for the first clinical trial of maraviroc.**

56. Gulick RM, Lalezari J, Goodrich J, et al. MOTIVATE Study Teams. Maraviroc for previously treated patients with R5 HIV-1 infection. N Engl J Med 2008;359:1429-41

57. Fatkenheuer G, Nelson M, Lazzarin A, et al. Subgroup analyses of maraviroc in previously treated R5 HIV-1 infection. N Engl J Med 2008;359:1442-55

58. What is Trofile™. Trofile-Monogram Biosciences. Available from: http://www.trofileassay.com/what_is_trofile.html [Last accessed 12 December 2011]

59. Perno CF, Craig C, Taylor S, et al. Efficacy and Viral Resistance Are Comparable when Maraviroc Is Administered Once Daily or Twice Daily with Boosted Protease Inhibitors in Treatment-experienced Patients [abstract PE7.3/4]. 13th European AIDS Conference; 12 – 15 October 2011; Belgrade, Serbia

60. Hardy D, Reynes J, Konourina I, et al. Efficacy and safety of maraviroc plus optimized background therapy in treatment-experienced patients infected with CCR5-tropic HIV-1: 48-week combined analysis of the MOTIVATE studies [abstract #792]. 15th Conference on Retroviruses and Opportunistic Infections; 3 – 6 February 2008; Boston, MA

61. Hoepelman IM, Ayoub A, Heera J. The incidence of severe liver enzyme abnormalities and hepatic adverse events in the Maraviroc Clinical Development Programme [abstract LBP7.9/1]. 11th European AIDS Conference/EACS; 24 – 27 October 2007; Madrid, Spain

62. Saag M, Ive P, Heera J, et al. A multicenter, randomized, double-blind,

comparative trial of a novel CCR5 antagonist, maraviroc versus efavirenz, both in combination with Combivir (zidovudine [ZDV]/lamivudine [3TC]), for the treatment of antiretroviral naive subjects infected with R5 HIV-1: week 48 results of the MERIT study [abstract #WESS104]. 4th IAS conference; 22 – 25 July 2007; Sydney, Australia

63. Cooper DA, Heera J, Goodrich J, et al. Maraviroc versus efavirenz, both in combination with zidovudine-lamivudine, for the treatment of antiretroviral-naive subjects with CCR5-tropic HIV-1 infection. J Infect Dis 2010;201:803-13

64. Heera J, Saag M, Ive P, et al. Virological correlates associated with treatment failure at week 48 in the phase III study of maraviroc in treatment naive patients [abstract #40LB]. 15th Conference on Retroviruses and Opportunistic Infections; 3 – 6 February 2008; Boston, MA

65. Hardy WD, Gulick RM, Mayer H, et al. Two-year safety and virologic efficacy of maraviroc in treatment-experienced patients with CCR5-tropic HIV-1 infection: 96-week combined analysis of MOTIVATE 1 and 2. J Acquir Immune Defic Syndr 2010;55:558-64

66. Sierra-Madero J, Di Perri G, Wood R, et al. Efficacy and safety of maraviroc versus efavirenz, both with zidovudine/lamivudine: 96-week results from the MERIT study. HIV Clin Trials 2010;11:125-32

67. Gulick RM, Su Z, Flexner C, et al. Phase 2 study of the safety and efficacy of vicriviroc, a CCR5 inhibitor, in HIV-1-Infected, treatment-experienced patients: AIDS clinical trials group 5211. J Infect Dis 2007;196:304-12

68. McCarthy MC, Suleiman J, Diaz R, et al. Vicriviroc Long-Term Safety and Efficacy: 96-Week Results from the VICTOR-E1 Study [abstract H-923]. 49th Interscience Conference on Antimicrobial Agents and Chemotherapy (ICAAC 2009); 12 – 15 September 2009; San Francisco, CA

69. Gathe J, Diaz R, Fatkenheuer G, et al. Phase III Trials of Vicriviroc in Treatment-experienced Subjects Demonstrate Safety but Not Significantly Superior Efficacy over Potent Background Regimens Alone [abstract 54LB]. 17th Conference on Retroviruses & Opportunistic Infections; 16 – 19 February 2010; San Francisco, CA

70. Nakata H, Maeda K, Miyakawa T, et al. Potent anti-R5-HIV-1 effects of a CCR5 antagonist AK602 in a novel hu-PBMC-Non-Obese-Diabetic-SCID, IL-2Rg-Chain-Knocked-Out AIDS mouse model. J Virol 2005;79:2087-96

71. Lalezari J, Thompson M, Kumar P, et al. Antiviral activity and safety of 873140, a novel CCR5 antagonist, during short-term monotherapy in HIV-infected adults. AIDS 2005;19:1443-8

72. Nichols WG, Steel HM, Bonny T, et al. Hepatotoxicity observed in clinical trials of aplaviroc (GW873140). Antimicrob Agents Chemother 2008;52:858-65

73. Demarest JF, Amrine-Madsen H, Irlbeck DM, Kitrinos KM; CCR102881 Clinical Study Team. Virologic failure in first-line human immunodeficiency virus therapy with a CCR5 entry inhibitor, aplaviroc, plus a fixed-dose combination of lamivudine-zidovudine: nucleoside reverse transcriptase inhibitor resistance regardless of envelope tropism. Antimicrob Agents Chemother 2009;53:1116-23

74. Cohen C, DeJesus E, Mills A, et al. Potent antiretroviral activity of the once-daily CCR5 antagonist INCB009471 over 14 days monotherapy [abstract TUAB106]. 4th IAS Conference on AIDS Pathogenesis, Treatment and Prevention; 22 – 25 July 2007; Sydney, Australia

75. Product Pipeline. Incyte Corp. Available from: http://www.incyte.com/drugs_product_pipeline.html [Last accessed 13 December 2011]

76. Klibanov OM, Williams SH, Iler CA. Cenicriviroc, an orally active CCR5 antagonist for the potential treatment of HIV infection. Curr Opin Investig Drugs 2010;11:940-50

77. Pipeline, Discovery & Development. Tobira Therapeutics. Available from: http://www.tobiratherapeutics.com/discovery.php [Last accessed 13 December 2011]

78. Westby M, Smith-Burchnell C, Mori J, et al. Reduced maximal inhibition in phenotypic susceptibility assays indicates that viral strains resistant to the CCR5 antagonist maraviroc utilize inhibitor-bound receptor for entry. J Virol 2007;81:2359-71

•• **In this study, detailed *in vitro* profile and mechanism of maraviroc resistance are shown.**

79. Pugach P, Marozsan AJ, Ketas TJ, et al. HIV-1 clones resistant to a small molecule CCR5 inhibitor use the inhibitor-bound form of CCR5 for entry. Virology 2007;361:212-28

80. LaBranche C, Kitrinos K, Howell R, et al. Clonal analysis of in vitro-derived viruses with reduced susceptibility to aplaviroc (873140, APL) shows wide ranges in IC50 and sequence changes [abstract 9]. Targeting HIV Entry—1st International Workshop; 2 – 3 December 2005; Bethesda, MD

81. Lewis M. A genotypic analysis of HIV-1 sequences from emerging resistant virus after in vitro serial passage with the CCR5 antagonist maraviroc (UK-427,857) [abstract 91]. 3rd European HIV Drug Resistance Workshop; 4 – 7 April 2005; Athens, Greece

82. Westby M. Maraviroc (MVC, UK-427,857)-resistant HIV-1 variants, selected by serial passage, are sensitive to CCR5 antagonists (GW873140, Schering-C, Schering-D) and T-20 (enfuvirtide) [abstract 65]. XIV International Drug Resistance Workshop; 7 – 11 June 2005; Quebec City, Canada

83. Craig C, Heera J, Lewis M, et al. Mechanisms of virologic failure with maraviroc in treatment-naive HIV-1-infected patients through 96 weeks [abstract 536]. 17th Conference on Retroviruses and Opportunistic Infections; 16 – 19 February 2010; San Francisco, CA

84. Waters L, Scourfield A, Marcano M, et al. The evolution of co-receptor tropism in patients interrupting suppressive HAART [abstract 439a]. 16th Conference on Retroviruses and Opportunistic Infections; 8 – 11 February 2009; Montreal, Canada

85. Whitcomb JM, Huang W, Fransen S, et al. Development and characterization of a novel single-cycle recombinant virus assay to determine human immunodeficiency virus type 1 coreceptor tropism. Antimicrob Agents Chemother 2007;51:566-75

86. Asmuth DM, Goodrich J, Cooper DA, et al. CD4+ T-cell restoration after

48 weeks in the maraviroc treatment-experienced trials MOTIVATE 1 and 2. J Acquir Immune Defic Syndr 2010;54:394-7

87. Cuzin L, Trabelsi S, Mouillot G, et al. ANRS 145 Marimuno Study: a Multi-centre Prospective Pilot Study Evaluating Intensification of Stable Antiviral Therapy with Maraviroc in HIV-1-infected Patients with Insufficient Immune Restoration Despite Persistently Controlled Viral Replication [abstract PS1/6]. 13th European AIDS Conference; 12 – 15 October 2011; Belgrade, Serbia

88. Dragic T, Trkola A, Thompson DA, et al. A binding pocket for a small molecule inhibitor of HIV-1 entry within the transmembrane helices of CCR5. Proc Natl Acad Sci USA 2000;97:5639-44

89. Tsamis F, Gavrilov S, Kajumo F, et al. Analysis of the mechanism by which the small-molecule CCR5 antagonists SCH-351125 and SCH-350581 inhibit human immunodeficiency virus type 1 entry. J Virol 2003;77:5201-8

90. Maeda K, Das D, Ogata-Aoki H, et al. Structural and molecular interactions of CCR5 inhibitors with CCR5. J Biol Chem 2006;281:12688-98

91. Maeda K, Das D, Yin P, et al. Involvement of the second extracellular loop and transmembrane residues of CCR5 in inhibitor binding and HIV-1 fusion: insights to mechanism of allosteric inhibition. J Mol Biol 2008;381:956-74

92. Kondru R, Zhang J, Ji C, et al. Molecular interactions of CCR5 with major classes of small-molecule anti-HIV CCR5 antagonists. Mol Pharmacol 2008;73:789-800

93. Shahlaei M, Madadkar-Sobhani A, Mahnam K, et al. Homology modeling of human CCR5 and analysis of its binding properties through molecular docking and molecular dynamics simulation. Biochim Biophys Acta 2011;1808:802-17

94. Garcia-Perez J, Rueda P, Alcami J, et al. Allosteric model of maraviroc binding to CC chemokine receptor 5 (CCR5). J Biol Chem 2011;286:33409-21

95. Hall SE, Mao A, Nicolaidou V, et al. Elucidation of binding sites of dual antagonists in the human chemokine receptors CCR2 and CCR5. Mol Pharmacol 2009;75:1325-36

96. Wu B, Chien EY, Mol CD, et al. Structures of the CXCR4 chemokine GPCR with small-molecule and cyclic peptide antagonists. Science 2010;330:1066-71

Affiliation

Kenji Maeda[†1] MD PhD, Debananda Das[1], Hirotomo Nakata[1,2] & Hiroaki Mitsuya[1,2]
[†]Author for correspondence
[1]National Cancer Institute,
Experimental Retrovirology Section,
HIV and AIDS Malignancy Branch,
9000 Rockville Pike,
Building 10, Room 5A11,
Bethesda, 20892. MD, USA
Tel: +1 301 496-9238;
Fax: +1 301 402 0709;
E-mail: maedak@mail.nih.gov
[2]Kumamoto University,
Graduate School of Biomedical Sciences,
Departments of Hematology & Infectious Diseases, Kumamoto 860-8556, Japan

Biochimica et Biophysica Acta 1830 (2013) 2917–2923

Contents lists available at SciVerse ScienceDirect

Biochimica et Biophysica Acta

journal homepage: www.elsevier.com/locate/bbagen

Albumin domain II mutant with high bilirubin binding affinity has a great potential as serum bilirubin excretion enhancer for hyperbilirubinemia treatment

Ai Minomo [a,1], Yu Ishima [a,b,1], Victor T.G. Chuang [c], Yoshiaki Suwa [d], Ulrich Kragh-Hansen [e], Toru Narisoko [a], Hiroshi Morioka [d], Toru Maruyama [a,b,*], Masaki Otagiri [a,f,g,**]

[a] Department of Biopharmaceutics, Graduate School of Pharmaceutical Sciences, Kumamoto University, Kumamoto, Japan
[b] Center for Clinical Pharmaceutical Science, Kumamoto University, Kumamoto, Japan
[c] School of Pharmacy, Curtin Health Innovation Research Institute, Curtin University, Perth, Australia
[d] Department of Analytical and Biophysical Chemistry, Graduate School of Pharmaceutical Sciences, Kumamoto University, Kumamoto, Japan
[e] Department of Biomedicine, University of Aarhus, DK-8000 Aarhus C, Denmark
[f] Faculty of Pharmaceutical Sciences, Sojo University, Kumamoto, Japan
[g] Drug Delivery System Research Institute, Faculty of Pharmaceutical Sciences, Sojo University, Kumamoto, Japan

ARTICLE INFO

Article history:
Received 9 October 2012
Received in revised form 14 December 2012
Accepted 7 January 2013
Available online 15 January 2013

Keywords:
Human serum albumin
Bilirubin
Liver failure
Hyperbilirubinemia
Phage display

ABSTRACT

Background: 4Z,15Z-bilirubin-IXα (BR), an endogenous toxic compound that is sparingly soluble in water, binds human serum albumin (HSA) with high affinity in a flexible manner. Our previous findings suggest that both Lys195 and Lys199 in subdomain IIA are important for the high-affinity binding of BR, and especially Lys199 in stand-alone domain II plays a prominent role in the renal elimination of BR. Our hypothesis is that HSA-domain II with high BR binding would be a useful therapeutic agent to treat hyperbilirubinemia in patients with impaired liver function.
Methods: Unbound BR concentrations were determined using a modified HRP assay. To evaluate the effect of pan3_3-13 domain II mutant in promoting urinary BR excretion, the serum concentration and urinary excretion amount of BR were determined using bile duct ligation mice.
Results: After three or six rounds of panning, pan3_3-13 and pan6_4 were found to have a significantly higher affinity for BR than wild-type domain II. Administration of pan3_3-13 significantly reduced serum BR level and increased its urinary excretion in the disease model mice as compared to wild-type domain II treatment.
Conclusions: These results suggest that pan3_3-13 has great potential as a therapeutic agent that promotes urinary BR excretion in hyperbilirubinemia.
General significance: This is the first study to be applied to other HSA bound toxic compounds that are responsible for the progression of disease, thereby paving the way for the development of non-invasive and cost effective blood purification treatment methods.

1. Introduction

Unconjugated bilirubin is poorly soluble in water at physiologic pH due to intramolecular hydrogen bonding shielding the hydrophilic sites of the bilirubin molecule, resulting in a hydrophobic structure. The fully hydrogen-bonded structure of bilirubin is designated 4Z,15Z-bilirubin-IXα (BR). This water-insoluble unconjugated BR is associated with all known toxic effects of BR. Thus, the internal hydrogen bonding is critical in producing bilirubin toxicity and also prevents its elimination. Disruption of the hydrogen bonds is essential to convert BR to a water-soluble form for elimination by the liver and kidney. This is normally achieved by glucuronidation in the liver. The resulting BR glucuronides are water-soluble and are readily excreted in bile and urine. However, if the liver's function is impaired conjugation of BR will not be possible, making the less efficient renal excretion to become the main route of elimination for the low water soluble unconjugated BR. As a result, the unconjugated bilirubin will accumulate in the blood and with high enough concentration encephalopathy will occur.

The main treatment for preventing BR-induced encephalopathy in newborns and especially in premature infants is phototherapy. Phototherapy converts BR, which primarily binds to HSA, into nontoxic structural isomers with higher water solubility that are more readily eliminated from the circulatory system via renal excretion [1]. The

Abbreviations: BR, 4Z,15Z-bilirubin-IXα; HSA, human serum albumin; BDL, bile duct ligation; SPR, surface plasmon resonance; WT, wild-type; HRP, horseradish peroxidase

* Correspondence to: T. Maruyama, Department of Biopharmaceutics, Graduate School of Pharmaceutical Sciences, Kumamoto University, Kumamoto, Japan.
** Correspondence to: M. Otagiri, Faculty of Pharmaceutical Sciences, Sojo University, Kumamoto, Japan.
E-mail addresses: tomaru@kumamoto-u.ac.jp (T. Maruyama), otagirim@ph.sojo-u.ac.jp (M. Otagiri).

[1] Both authors contributed equally.

0304-4165/$ – see front matter © 2013 Elsevier B.V. All rights reserved.
http://dx.doi.org/10.1016/j.bbagen.2013.01.006

rate of isomers formation and the isomeric composition of the reaction products have been shown to be highly dependent on the conformation and electronic environment of BR bound to HSA [2,3]. We have shown in a previous study that the P-form of BR is more readily converted into photoisomers with higher water solubility than the M-form, and that the P-form binds preferentially to HSA [4]. Indeed, a 5% albumin infusion has been shown in a randomized controlled clinical trial to be effective in reducing unconjugated serum bilirubin levels in low birth weight neonates with intensive phototherapy failure [5].

However, phototherapy is not without unwanted consequences [6]. The most common complication reported so far is a high incidence of squints and abnormal developmental performance in infants treated with phototherapy, suggesting that phototherapy should not be used indiscriminately for hyperbilirubinemia until the results of further long-term studies are available. Most importantly, the prevention of kernicterus and neurotoxic effect of bilirubin, particularly in the low birth weight newborn, needs to be achieved within the shortest time possible.

Although HSA binds bilirubin with high affinity, without phototherapy it cannot effectively eliminate the bound toxin via renal excretion because HSA possesses a large molecular weight that leads to long blood retention and normally no excretion in the urine [7]. In this regard, an HSA domain with only one third of the whole HSA molecular weight (HSA has three domains) should have higher clearance from the blood circulation. In a previous study, we reported that individual recombinant domains including domain II that contains the bilirubin binding site showed about 50-fold faster total clearance than HSA [8]. Similar observations have been reported by Sheffield et al. using recombinant domains of rabbit serum albumin [9]. This indicates that HSA-domain II with conserved Lys199 would be useful in treating jaundiced newborns, because it can preferentially bind the P-form of BR with a comparable high affinity, and more importantly it could be cleared from the body via the kidney without the aid of phototherapy. Taken together, our hypothesis about toxin removal therapy by albumin domains is illustrated in Fig. 1.

However, Matsushita et al. reported that ligand binding ability of the recombinant HSA domains decreased compared with HSA [8]. Therefore, we first identified key amino acid residues that contribute to high affinity binding of BR by phage library based on previous reports on BR binding site and constructed HSA mutant domain accordingly [4].

Then, we demonstrated the effect of HSA mutant domain on BR binding ability and its elimination *in vitro* and *in vivo*. The present work laid the groundwork for development of new therapeutic agents for treating jaundiced newborns.

2. Experimental section

2.1. Measurement of free BR concentration–horseradish peroxidase (HRP) assay

All absorption measurements in this study were recorded with a model 680 microplate reader (Bio-Rad Laboratories, Inc). Unbound BR concentrations were determined using a modification of the HRP

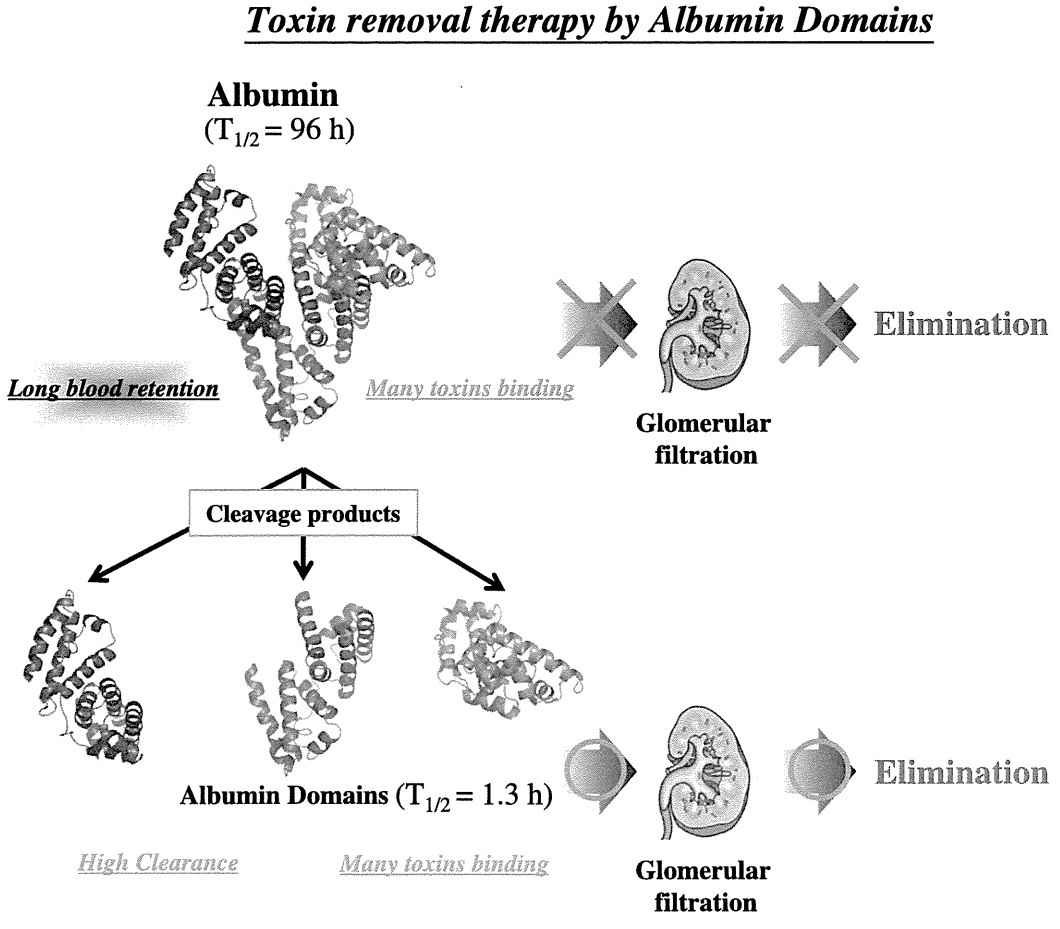

Fig. 1. The concept of toxin removal therapy by albumin domains. HSA cannot eliminate albumin binding toxins because HSA possesses long blood retention in Human and is normally not excreted in urine. On the other hand, individual HSA domains with not only many toxin binding sites but also high clearance from blood circulation could eliminate these toxins, indicating that HSA domains apply for toxin removal therapy. The half-lives given are for the mouse.

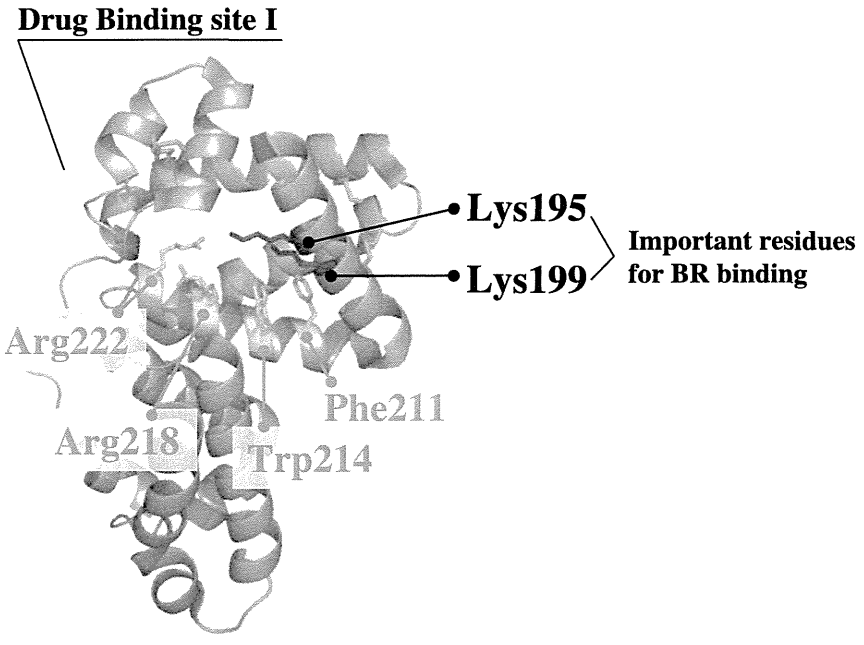

Fig. 2. Substitution sites of a phage library displaying recombinant HSA domain II.

assay [4]. 60 μM BR was added to 30 μM recombinant domain II clones dissolved in 67 mM phosphate buffer (pH 7.4). The concentration of unbound BR is below 35 μM in these solutions. 200 μl aliquots of the BR/protein complexes were placed in a 96 well-plate and the samples allowed to equilibrate for 20 min at 37 °C. 10 μL of freshly diluted 1.75 mM hydrogen peroxide was added to each well, followed by incubation for 3 min. The reaction was initiated by adding 10 μL of 1 ng/mL HRP. The rate of oxidative destruction of unbound BR was monitored by the reduction in the absorbance of the mixture at 450 nm for 10 min. The concentrations of unbound BR were determined by extrapolating the rate of oxidation of BR to a standard curve prepared by plotting oxidation rate versus BR concentration. It was assumed that only unbound BR was available as a substrate for HRP so that there was a linear relationship between the rate of destruction of BR and the concentration of unbound species.

Table 1
Partial amino acid sequences of HSA-domain II clones selected after three (A) or six (B) rounds of panning on BR.

(A)

	211 214 218 222
WT	QKFGERAFKAWAVARLSQRFPKAEFAEVS
1-5	QKFGERAVKAQAVAELSQVFPKAEFAEVS
1-6	QKFGERALKAWAVASLSQWFPKAEFAEVS
1-8	QKFGERAVKAQAVAELSQVFPKAEFAEVS
1-9	QKFGERAQKATAVAALSQAFPKAEFAEVS
1-10	QKFGERATKAVAVARLSQVFPKAEFAEVS
2-1	QKFGERARKALAVAKLSQSFPKAEFAEVS
2-2	QKFGERAWKAKAVALLSQMFPKAEFAEVS
2-3	QKFGERARKAKAVAALSQPFPKAEFAEVS
2-4	QKFGERARKAMAVANLSQQFPKAEFAEVS
2-6	QKFGERARKARAVAVLSQGFPKAEFAEVS
2-7	QKFGERAIKAAAVAQLSQGFPKAEFAEVS
2-9	QKFGERAMKAQAVAALSQTFPKAEFAEVS
2-10	QKFGERAAKADAVASLSQQFPKAEFAEVS
2-11	QKFGERASKARAVASLSQAFPKAEFAEVS
2-12	QKFGERAMKASAVAYLSQWFPKAEFAEVS
2-13	QKFGERARKAGAVATLSQFFPKAEFAEVS
2-14	QKFGERALKADAVASLSQGFPKAEFAEVS
3-1	QKFGERAQKAFAVAVLSQLFPKAEFAEVS
3-2	QKFGERAWKARAVATLSQRFPKAEFAEVS
3-3	QKFGERAPKALAVAILSQGFPKAEFAEVS
3-5	QKFGERAPKATAVAVLSQQFPKAEFAEVS
3-6	QKFGERAYKAGAVASLSQGFPKAEFAEVS
3-7	QKFGERAVKAFAVAFLSQQFPKAEFAEVS
3-9	QKFGERAQKAQAVARLSQGFPKAEFAEVS
3-10	QKFGERAGKARAVAGLSQFFPKAEFAEVS
3-11	QKFGERATKAWAVATLSQQFPKAEFAEVS
3-13	QKFGERARKAWAVALLSQRFPKAEFAEVS
3-15	QKFGERAAKAYAVAQLSQYFPKAEFAEVS

(B)

	211 214 218 222
WT	QKFGERAFKAWAVARLSQRFPKAEFAEVS
2	QKFGERAFKAWAVAALSQGFPKAEFAEVS
4	QKFGERALKAWAVASLSQWFPKAEFAEVS
5	QKFGERAWKAWAVATLSQEFPKAEFAEVS
6	QKFGERALKAWAVASLSQWFPKAEFAEVS
7	QKFGERASKAQAVAWLSQCFPKAEFAEVS
8	QKFGERALKAWAVASLSQWFPKAEFAEVS
9	QKFGERAQKAQAVARLSQWFPKAEFAEVS
10	QKFGERALKAWAVASLSQWFPKAEFAEVS
11	QKFGERALKAWAVASLSQWFPKAEFAEVS
12	QKFGERAFKAWAVAALSQWFPKAEFAEVS
14	QKFGERAFKAWAVAALSQWFPKAEFAEVS
15	QKFGERALKAWAVASLSQWFPKAEFAEVS
16	QKFGERAFKADAVARLSQHFPKAEFAEVS
19	QKFGERALKAWAVATLSQWFPKAEFAEVS
23	QKFGERALKAWAVASLSQWFPKAEFAEVS
24	QKFGERAQKATAVARLSQWFPKAEFAEVS
26	QKFGERALKAWAVASLSQWFPKAEFAEVS
27	QKFGERALKAWAVASLSQWFPKAEFAEVS
28	QKFGERALKAWAVASLSQWFPKAEFAEVS
29	QKFGERALKAWAVASLSQWFPKAEFAEVS
30	QKFGERALKAWAVASLSQWFPKAEFAEVS
31	QKFGERALKAWAVASLSQWFPKAEFAEVS
32	QKFGERALKAWAVASLSQWFPKAEFAEVS
33	QKFGERAVKARAVAQLSQQFPKAEFAEVS
34	QKFGERALKARAVADLSQWFPKAEFAEVS
35	QKFGERALKARAVADLSQWFPKAEFAEVS
36	QKFGERALKARAVADLSQWFPKAEFAEVS

2.2. Surface plasmon resonance (SPR) measurements

The binding of BR to recombinant HSA-domain II (WT and pan3_3_13) was measured by a Biacore T100 system at 25 °C and a flow rate of 30 μL/min. Recombinant HSA-domain II (5000 ± 500 response units) was immobilized on a CM5 surface. A CM5 chip was activated using 1:4 *N*-hydroxysuccinimide/1-ethyl-3-(3-dimethylaminopropyl) carbodiimide at a flow rate of 10 μL/min for 7 min. HSA (50 μg/mL) in 10 mM acetate buffer (pH 4.5) was passed over separate flow cells at 10 μL/min for 7 min, and this was followed by a blocking step using ethanolamine (1 M, pH 8.5) at 10 μL/min for 7 min. Binding studies were performed by passing BR over the immobilized recombinant HSA-domain II (WT and pan3_3_13) at a flow rate of 30 μL/min. The association and dissociation times were 120 and 360 s, respectively.

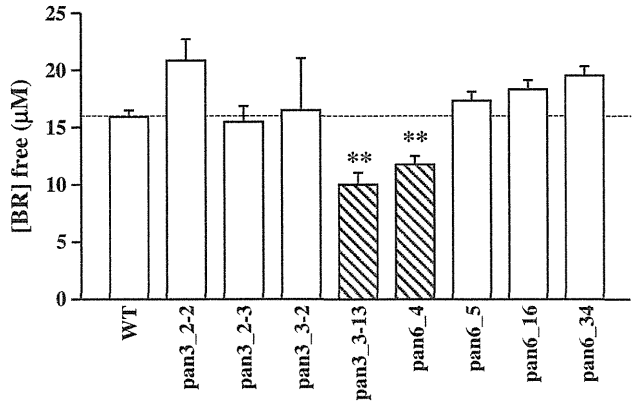

Fig. 3. BR-binding properties of HSA-domain II clones. The concentration of unbound BR in the presence of recombinant domain II was determined by the HRP assay. BR at 60 μM was incubated with 30 μM recombinant domain II clones, each dissolved in 67 mM phosphate buffer (pH 7.4). Data are expressed as means ± SD of the mean (n = 3). **$P<0.01$, as compared with the corresponding WT.

Table 2
Partial amino acid sequences of domain II WT, pan3_3-13 and pan6-4.

residue	211 214 218 222
WT	GERAFKAWAVARLSQRFPKA
pan3_3-13	GERARKAWAVALLSQRFPKA
pan6_4	GERALKAWAVASLSQWFPKA

The running buffer contained PBS and 5% DMSO. The complex formation between BR and the immobilized protein was measured with 0.5–1.2 μM of ligand in the running buffer. A sample volume of 60 μL was injected into the flow cell. Dissociation of the bound ligand was initiated by injecting 10 mM NaOH for 15 s.

2.3. In vivo evaluation of the urinary bilirubin excretion promoting activity of pan3_3-13

This experiment was carried out after permission was granted by the Committee of Animal Experimentation of Kumamoto University. Humane animal care and use was performed according to the Guideline for Animal Experiments at Kumamoto University. The male mice were ICR, 7 weeks of age. Common bile duct ligation (BDL) was performed on the mice using a method previously described [10]. Briefly, mice were anesthetized and the peritoneal cavity opened. The common bile duct was exposed and ligated with No. 2 black silk suture. After 4 days of bile duct ligation, the animal was anesthetized again to collect blood samples for BR concentration determinations. The BR value was measured with an automatic analyzer (FDC4000; Fuji Medical Systems, Tokyo, Japan). After randomization-based on the following reason: the range of plasma BR concentrations were 2–20 mg/dL, HSA or domain II proteins were administrated intravenously via the tail vein. At 2 h after the administration, blood samples were collected to measure BR concentration.

3. Results

3.1. Design of HSA-domain II mutants

We have previously created pCANTAB 5E phagemid vector encoding HSA-domain II (residues 187–385) [4]. Based on this phagemid vector, we constructed a phage library displaying mutated BR binding site on HSA-domain II (Fig. 2). In a previous study, we have reported that Lys195 and Lys199 are two key residues that interact with the carboxyl groups of BR via salt bridge formation [4]. Therefore, in this study we focused on identifying hydrophobic amino acid residues around Lys195 and Lys199 that are present in a drug binding pocket called site I.

Table 3
Dissociation and kinetics constants of BR-domain II complex.

	K_D(M)	k_{a1}(1/Ms)	k_{d1}(1/s)	k_{a2}(1/Ms)	k_{d2}(1/s)
WT	1.5×10^{-6}	1.8×10^{4}	2.8×10^{-2}	–	–
pan3_3-13	0.23×10^{-6}	1.5×10^{4}	3.8×10^{-2}	4.6×10^{-3}	4.4×10^{-4}

3.2. Phage display selection of recombinant HSA-domain II with high binding affinity for BR

In order to identify the recombinant domain II-displaying phages with high BR binding affinities, the phage library was subjected to three or six rounds of panning against BR immobilized on an EAH Sepharose 4E gel as described in Supplementary information. After the third and sixth panning, 28 and 27 phage clones were isolated, respectively. Among these 28 clones from the third panning, the same amino acid sequence could not be found. However, 16 of 27 phage clones from the sixth panning possess homologous sequences (Table 1). Next, we randomly selected 4 clones from the third and the sixth panning groups for protein expression using the *Pichia pastoris* protein expression system [11].

3.3. Evaluation of BR binding capacity of the selected clones

To identify the domain II mutant with the highest BR binding affinity, the 8 domain II mutants were expressed with the *Pichia pastoris* protein expression system and purified. Their BR binding capabilities were then evaluated with the HRP assay. As can be seen in Fig. 3, 6 of the 8 domain II mutants bound BR equally well and with an affinity comparable to that of wild-type (WT) domain II. Intriguingly, the other two mutants (pan3_3-13 and pan6_4) had significantly higher BR binding affinity than WT domain II (Fig. 3). DNA sequencing analysis showed that both pan3_3-13 and pan6_4 had the same amino acid, tryptophan, as the WT domain II at position 214, but the amino acid at position 218 had been mutated to an amino acid with shorter side chain such as Leu or Ser, suggesting that the binding pocket in these two domain II mutants was almost conserved but the entrance to the binding pocket was bigger than in WT (Table 2). In order to clarify the binding to the domain II mutants and the structural characterization

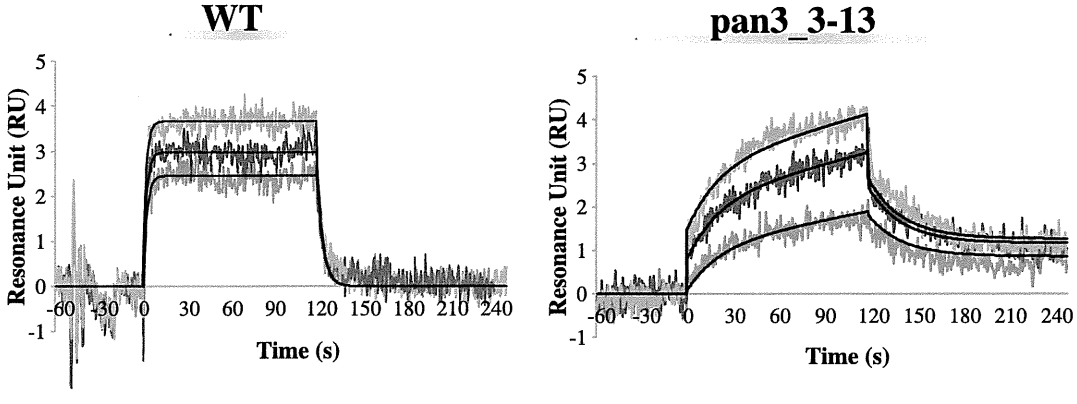

Fig. 4. Sensorgram curves of BR on WT domain II and pan3_3-13. All data were collected on BIACORE T100. Binding studies were performed by passing BR over the immobilized recombinant HSA-domain II (WT and pan3_3_13) at a flow rate of 30 μL/min. The complex formation between BR and the immobilized protein was measured with 0.5–1.2 μM of ligand in the running buffer. A sample volume of 60 μL was injected into the flow cell. Dissociation of the bound ligand was initiated by injecting 10 mM NaOH for 15 s.

1:1 binding

$$A + B \underset{k_{d1}}{\overset{k_{a1}}{\rightleftharpoons}} AB$$

Two state reaction

$$A + B \underset{k_{d1}}{\overset{k_{a1}}{\rightleftharpoons}} \underset{\textit{Initial complex}}{AB} \underset{k_{d2}}{\overset{k_{a2}}{\rightleftharpoons}} \underset{\textit{Stable complex}}{(AB)^*}$$

Scheme 1. Dissociation constants of 1:1 binding and two state reaction model.

of these domain II mutant-BR complexes, we focused on pan3_3-13 which possesses the highest BR binding affinity according to the HRP method (Fig. 3).

3.4. Binding and structural characterization of the selected HSA-domain II clone-BR complex

Fig. 4 shows the binding characterization of BR to WT and pan3_3-13 using Biacore analysis. The results showed that the BR binding affinity of pan3_3-13 was about 7 times higher than that of WT (Fig. 4, Table 3). Interestingly, these sensorgrams showed that pan3_3-13 binds BR via a different binding manner from that of WT. The BR binding manner by WT can be described with a simple 1:1 bimolecular reaction, whereas that for pan3_3-13 can be described with a two-state reaction model (Scheme 1), indicating that the binding of pan3_3-13 to bilirubin involves either a sequential two-step process or some conformational changes. It is difficult to draw conclusion from only comparing the k_{a1} and k_{d1} values of WT and pan3_3-13, because their best fitted binding models are quite different.

The response curves of various analyte concentrations were globally fitted to either the 1:1 Langmuir model or the two-state binding model (Scheme 1) where the equilibrium constants of each binding step are $K_1 = k_{a1}/k_{d1}$ and $K_2 = k_{a2}/k_{d2}$, and the overall equilibrium binding constant is calculated as $K_A = K_1(1/K_2)$ and $K_d = 1/K_A$. In this model, the analyte (A) binds to the ligand (B) to form an initial complex (AB) and then undergoes subsequent binding or conformational change to form a more stable complex (AB)*. Generally, the interaction accompanied by a conformational change results in a better fit and stronger binding [12,13].

Furthermore, we constructed the structure of WT-BR and pan3_3-13-BR complexes with docking simulation (Fig. 5). The result showed that the entrance of BR-binding pocket in pan3_3-13 has expanded by the replacement of Arg with Leu at position 218, suggesting that BR could enter the pocket more deeply as compared with WT.

3.5. In vivo evaluation of urinary BR excretion promoting effect of pan3_3-13

In order to evaluate the potential of pan3_3-13 as a therapeutic agent in treating hyperbilirubinemia, the effects of pan3_3-13 administration on the BR serum concentration and urinary excretion of BR were examined using BDL mice. Administration of saline or HSA increased the serum bilirubin level of the BDL mice (Figs. 6 and 7). These data indicate that pathology of BDL is in progress. In contrast, administration of wild-type domain II significantly reduced serum bilirubin level in the mice (Figs. 6 and 7). It is postulated that domain II promoted BR excretion into urine by its high affinity binding of the toxin.

This suggestion is supported by the increased urinary BR concentration (Fig. 8). Moreover, as expected from the increased binding affinity, administration of pan3_3-13 significantly reduced serum bilirubin level and increased bilirubin excretion compared to wild-type domain II treatment. The degree of urinary bilirubin excretion was in order of

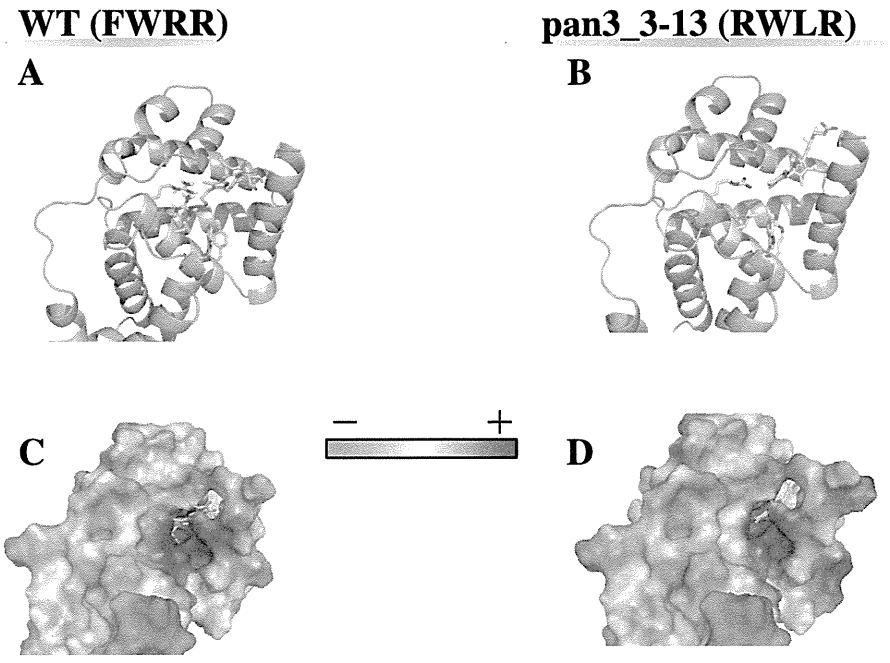

Fig. 5. Structure prediction by molecular dynamics simulation. Ribbon diagram of domain II (A) and pan3_3-13 (B) with 4Z, 15E-BR. 211, 214, 218 and 222-residues and 4Z, 15E-BR are shown in green (A) or yellow (B). Stereo view of an electrostatic surface of domain II (C) and pan3_3-13 (D) with 4Z, 15E-BR, showing the basic pocket on the concave of the molecule. Acidic and basic residues are colored red and blue, respectively.

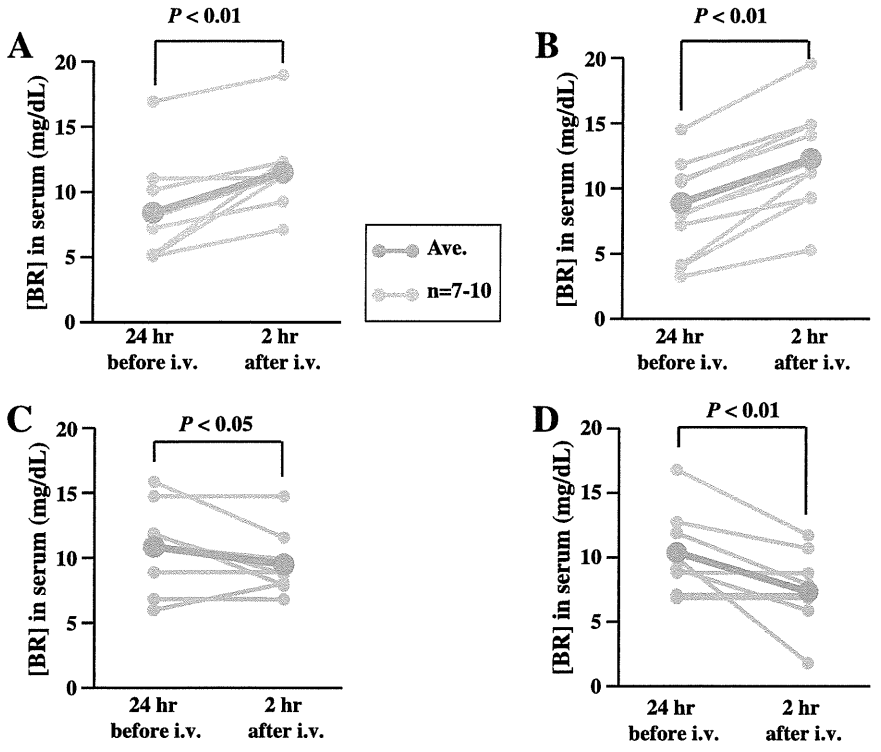

Fig. 6. Plasma concentrations of BR. Plasma concentrations of BR at 2 hr after administration of saline (A), HSA (30 mg/kg) (B), domain II (30 mg/kg) (C) and pan3_3-13 (30 mg/kg) (D) (n = 7–10). Mean concentrations of total BR were showed as red lines.

pan3_3-13 > wild-type domain II > saline or HSA treatment. In addition, western blotting data showed that pan3_3-13 was excreted by 9 h after administration (Fig. 8).

4. Discussion

Our study has performed two major investigations. First, we selected recombinant HSA-domain II with high binding affinity for BR using phage display technology. We hypothesized that the van der Waals radii of this pocket might need to change in order to construct a HSA-domain II mutant with high and increased binding affinity for BR. To test this hypothesis, Phe211, Trp214, Arg218 and Arg222 from a neighboring helix with their side chains orientated in the same direction as those of Lys195 and Lys199 were mutated. To produce these substitutions, the codons of these four residues were replaced with NNS (where N and S represent A/G/C/T and G/C respectively). NNS encodes all possible amino acid substitutions while limiting the total number of codons to 32. The sequences of unselected phages

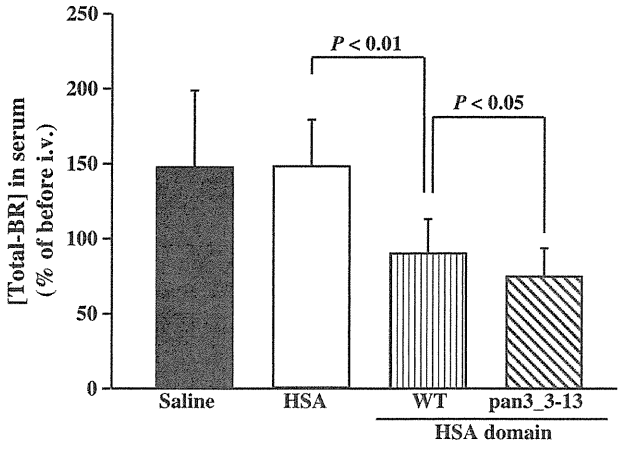

Fig. 7. Relative plasma concentrations of BR. Plasma concentrations of BR at 2 hr after administration of proteins.

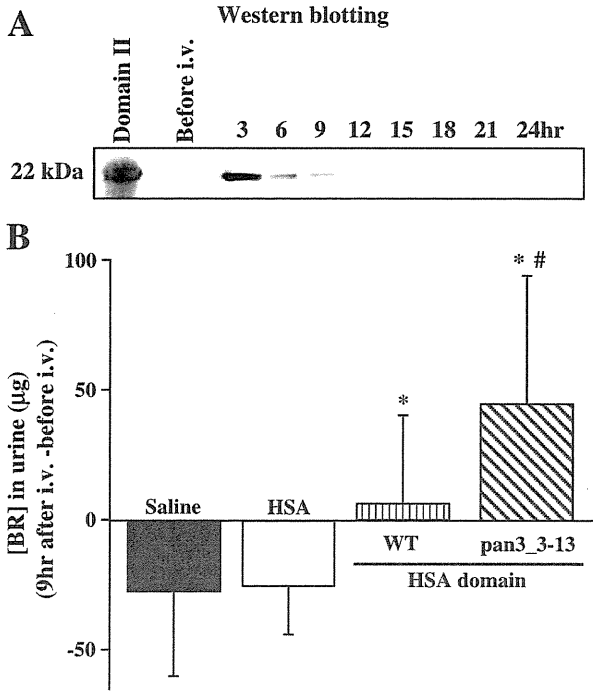

Fig. 8. The urinary excretion analysis of exogenous domain II by Western blotting and Relative Urine concentrations of BR. (A) The excretion of exogenous domain II in urine at 3, 6, 9, 12, 15, 18, 21 and 24 hr after i.v. administration of domain II were detected by Western blotting using anti-HSA polyclonal antibody. (B) The excretion of total BR in urine until 9 hr after i.v. administration of domain II proteins. *$P<0.05$, as compared with saline or HSA, #$P<0.05$,as compared with WT.

displayed little or no bias (data not shown). The library contained approximately 1.6×10^5 phage clones, a size that covers all potential clones that can be expressed. In order to identify the recombinant domain II-displaying phages with high BR binding affinities, the phage library was subjected to three or six rounds of panning. As the result, we could success to get two mutants (pan3_3-13 and pan6_4) with high BR binding affinities.

Second, we performed the BDL mice study to evaluate the potential of pan3_3-13 as a therapeutic agent in treating hyperbilirubinemia. The Domain II mutant of pan3_3-13 for *in vivo* study was expressed by the *Pichia pastoris* protein expression system. Treatment of HSA, which possesses normally no excretion in the urine, did not affect serum BR concentration in BDL mice. On the other hand, Treatment of pan3_3-13, which possesses high BR binding affinities and excretion in the urine, could significantly decrease serum BR concentration compared with HSA treatment. The dose-dependency of domain II in BR excretion therapy has also been examined (Supplementary Fig. 1). These results proposed that pan3_3-13 could function as a therapeutic agent that promotes urinary bilirubin excretion in hyperbilirubinemia.

The present work points to possible novel treatment option for hyperbilirubinemia. It is 'Albumin Domains Therapy'. Sheffield et al. produced recombinant versions of domain I, I+II and III of rabbit serum albumin, and found that all three "miniproteins" were eliminated very rapidly from rabbits by a renal route; the mean terminal catabolic half-life for all the "miniproteins" was less than 0.071 days, but it was 4.32 days for the full body protein [9]. Moreover, we previously performed that cyanogen bromide (CNBr) cleavage of HSA under non-reduced condition will produce 3 peptides, one of which is the 20 kDa fragment that contains domain II. A preliminary study has been conducted to examine the effect of HSA and the 20 kDa CNBr fragment of HSA on the renal excretion of BR in rats. Rats were intravenously administered with either BR alone, BR and HSA mixture or 20 kDa fragment mixture. Rats administered with the 20 kDa fragment showed a higher renal clearance of BR compared to those administered with HSA, since the urine BR concentration after 120 minutes for the 20 kDa fragment group was about two fold higher than that of the HSA group. In addition, the protein concentration in urine also showed similar tendency whereby the 20 kDa fragment group concentration was about two fold higher than that of the whole HSA group [4]. These data are congruent with this present study.

5. Conclusions

Using phage display technology, the present study identifies amino acid residues of HSA that are important for high-affinity binding of BR. Based on the results, individual HSA domain II mutants with high BR binding affinity was produced. To our knowledge, this is the first report on HSA mutant domain with enhanced binding affinity to BR. This approach could be applied to other HSA bound toxic compounds that are responsible for the progression of disease, thereby paving the way for the development of non-invasive and cost effective blood purification treatment methods. In conclusion, pan3_3-13 could function as a therapeutic agent that promotes urinary bilirubin excretion in hyperbilirubinemia.

Acknowledgments

This research was supported by Grant-in-Aid for Scientific Research from Japan Society for the Promotion of Science (JSPS) (KAKENHI 18390051 and 22790162). The work was also in part supported by grants from KUMAYAKU Alumni Research Fund. We thank Tomohiro Horiuchi and Eriko Kasamo, Kumamoto University for technical assistance. We are grateful to Dr. Ayaka Suenaga, Kumamoto University for helpful discussions. Thanks also go to members of the Gene Technology Center in Kumamoto University for their important contributions to the experiments.

Appendix A. Supplementary data

Supplementary data to this article can be found online at http://dx.doi.org/10.1016/j.bbagen.2013.01.006.

References

[1] M.J. Maisels, A.F. McDonagh, Phototherapy for neonatal jaundice, N. Engl. J. Med. 358 (2008) 920–928.
[2] C.E. Petersen, C.E. Ha, K. Harohalli, J.B. Feix, N.V. Bhagavan, A dynamic model for bilirubin binding to human serum albumin, J. Biol. Chem. 275 (2000) 20985–20995.
[3] M.M. Khan, S. Muzammil, S. Tayyab, Role of salt bridge(s) in the binding and photoconversion of bilirubin bound to high affinity site on human serum albumin, Biochim. Biophys. Acta 1479 (2000) 103–113.
[4] A. Minomo, Y. Ishima, U. Kragh-Hansen, V.T.G. Chuang, M. Uchida, K. Taguchi, H. Watanabe, T. Maruyama, H. Morioka, M. Otagiri, Biological characteristics of two lysines on human serum albumin in the high-affinity binding of 4Z,15Z-bilirubin-IXalpha revealed by phage display, FEBS J. 278 (2011) 4100–4111.
[5] S. Mitra, M. Samanta, M. Sarkar, A.K. De, S. Chatterjee, Pre-exchange 5% albumin infusion in low birth weight neonates with intensive phototherapy failure—a randomized controlled trial, J. Trop. Pediatr. 57 (2011) 217–221.
[6] J.H. Drew, K. Marriage, V.V. Bayle, E. Bajraszewski, J.M. McNammara, Phototherapy. Short and long-term complications, Arch. Dis. Child. 51 (1976) 454–458.
[7] T. Peters Jr., The Albumin Molecule: Its Structure and Chemical Properties, All About Albumin: Biochemistry, Genetics, and Medical Applications, Academic Press, San Diego, CA, 1996, pp. 9–75.
[8] S. Matsushita, Y. Isima, V.T.G. Chuang, H. Watanabe, S. Tanase, T. Maruyama, M. Otagiri, Functional analysis of recombinant human serum albumin domains for pharmaceutical applications, Pharm. Res. 21 (2004) 1924–1932.
[9] W.P. Sheffield, J.A. Marques, V. Bhakta, I.J. Smith, Modulation of clearance of recombinant serum albumin by either glycosylation or truncation, Thromb. Res. 99 (2000) 613–621.
[10] M. Song, Z. Song, S. Barve, J. Zhang, T. Chen, M. Liu, G.E. Arteel, G.J. Brewer, C.J. McClain, Tetrathiomolybdate protects against bile duct ligation-induced cholestatic liver injury and fibrosis, J. Pharmacol. Exp. Ther. 325 (2008) 409–416.
[11] H. Watanabe, K. Yamasaki, U. Kragh-Hansen, S. Tanase, K. Harada, A. Suenaga, M. Otagiri, In vitro and in vivo properties of recombinant human serum albumin from pichia pastoris purified by a method of short processing time, Pharm. Res. 18 (2001) 1775–1781.
[12] M. Futamura, P. Dhanasekaran, T. Handa, M.C. Phillips, S. Lund-Katz, H. Saito, Two-step mechanism of binding of apolipoprotein E to heparin: implications for the kinetics of apolipoprotein E-heparan sulfate proteoglycan complex formation on cell surfaces, J. Biol. Chem. 280 (2005) 5414–5422.
[13] T.A. Morton, D.G. Myszka, I.M. Chaiken, Interpreting complex binding kinetics from optical biosensors: a comparison of analysis by linearization, the integrated rate equation, and numerical integration, Anal. Biochem. 227 (1995) 176–185.

Pharmaceutical Aspects of the Recombinant Human Serum Albumin Dimer: Structural Characteristics, Biological Properties, and Medical Applications

KAZUAKI TAGUCHI,[1] VICTOR TUAN GIAM CHUANG,[2] TORU MARUYAMA,[1,3] MASAKI OTAGIRI[1,4,5]

[1]Department of Biopharmaceutics, Graduate School of Pharmaceutical Sciences, Kumamoto University, Kumamoto 862-0973, Japan

[2]School of Pharmacy, Faculty of Health Sciences, Curtin Health Innovation Research Institute, Curtin University, Perth 6845, Western Australia, Australia

[3]Center for Clinical Pharmaceutical Sciences, Kumamoto University, Kumamoto 862-0973, Japan

[4]Faculty of Pharmaceutical Sciences, Sojo University, Kumamoto 860-0082, Japan

[5]DDS Research Institute, Sojo University, Kumamoto 860-0082, Japan

Received 14 February 2012; revised 12 April 2012; accepted 18 April 2012

Published online 9 May 2012 in Wiley Online Library (wileyonlinelibrary.com). DOI 10.1002/jps.23181

ABSTRACT: Human serum albumin is the most abundant protein in the blood. It is clinically used in the treatment of severe hypoalbuminemia and as a plasma expander. The use of albumins as a carrier for drugs is currently being developed, and some are now in the preclinical and clinical trial stages. The main technologies for utilizing an albumin as a drug carrier are protein fusion, polymerization and surface modification, and so on. Among these technologies, albumin dimerization has wide clinical applications as a plasma expander as well as a drug carrier. Despite the fact that many reports have appeared on drugs using an albumin dimer as a carrier, our knowledge of the characteristics of the albumin dimer itself is incomplete. In this review, we summarize the structural characteristics of recombinant albumin dimers produced by two methods, namely, chemical linkage with 1,6-bis(maleimido)hexane and genetically linked with an amino acid linker, and the physicochemical characteristics and biological properties of these preparations. Finally, the potential for pharmaceutical applications of albumin dimers in clinical situations is discussed. © 2012 Wiley Periodicals, Inc. and the American Pharmacists Association J Pharm Sci 101:3033–3046, 2012

Keywords: albumin; biomaterials; disposition; drug delivery systems; nanotechnology; physicochemical properties; polymeric biomaterials

INTRODUCTION

Human serum albumin (HSA) is a single-chain protein comprises 585 amino acids, is synthesized in the liver, and is the most abundant protein in the blood. On the basis of X-ray crystallographic analyses of recombinant HSA (rHSA), the polypeptide chain is organized into three homogeneous domains and forms a heart-shaped structure with dimensions of 80 × 80 × 80 Å^3 (Fig. 1).[1] HSA transports numerous endogenous and exogenous compounds such as fatty acids, hormones, toxic metabolites, bile acids, amino acids, drugs, and metals.[2,3] In addition, HSA contains a single thiol group from an unpaired cysteine residue at position 34 (Cys34). Cys34 in domain I of HSA provides antioxidant activity and constitutes the largest fraction of free thiol groups in the blood.[4] This antioxidant activity of HSA influences the plasma thiol-dependent antioxidant status as well as levels of oxidative damage to proteins.[5,6] Furthermore, because HSA is responsible for 80% of the colloid osmotic pressure of plasma (25–33 mmHg), a reduction in the concentration of HSA in the blood circulation

Abbreviations used: HSA, human serum albumin; rHSA, recombinant HSA; Cys34, cysteine at position 34; $t_{1/2}$, half-life; BMH, 1,6-bis(maleimido)hexane; CD, circular dichrosim; T_d, denaturing temperature; ΔH, enthalpy change during the denaturation; T_m, denaturation temperature; ΔH_m, enthalpy of transition; RBCs, red blood cells; NphOAc, *p*-nitrophenyl acetate; CMPF, 3-carboxy-4-methyl-5-propyl-2-furanpropanic acid; rRSA, recombinant rabbit serum albumin; GLP-1, glucagon-like 1 peptide; EPR, enhanced permeability and retention; NO, nitric oxide; SNO-dimer, *S*-nitrosated genetic rHSA-dimer; FecycP, 2-[8-{N-(2-methylimidazolyl)}octanoyloxymethyl]-5,10,15,20-tetrakis{α,α,α,α-*o*-(1-methylcyclohexanamido)phenyl}porphinatoiron(II).

Correspondence to: Masaki Otagiri (Telephone: +81-96-326-3887; Fax: +81-96-326-3887; E-mail: otagirim@ph.sojo-u.ac.jp)

Journal of Pharmaceutical Sciences, Vol. 101, 3033–3046 (2012)

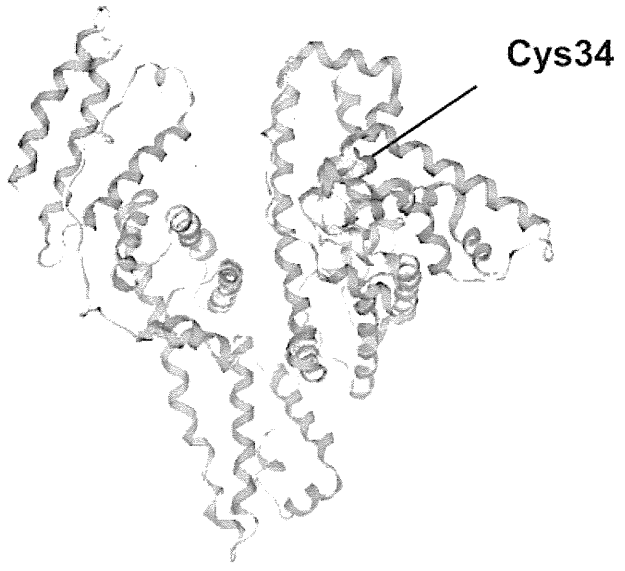

Figure 1. Crystal structure of human serum albumin showing the location of Cys34.

results in edema, ascites, and pleural effusion. Clinically, HSA is used as a plasma expander, and the administration of HSA is generally considered to be the gold standard for treating severe hypoalbuminemia as a result of conditions such as burns, the nephritic syndrome, reduction in the synthesis of HSA induced by chronic liver cirrhosis, and hemorrhagic shock.

In addition to the use of HSA alone, drugs that can be transported in conjunction with HSA have been recently approved by many countries and provide beneficial effects. For example, Abraxane® (American Bioscience, Los Angeles, CA), which is an albumin–paclitaxel nanoparticle with a mean particle size of 130 nm, was approved for the treatment of metastatic breast cancer. Albumin and paclitaxel, in the form of a complex, have several beneficial effects; Abraxane® accumulates in tumors through the enhanced permeability and retention (EPR) effect of solid tumors, but a further albumin transport pathway mediated by gp60 located on the surface of endothelial cells appears to be responsible for the tumor uptake and tumor distribution of Abraxane® and the subsequent release of paclitaxel.[7–9] Several drugs and agents that use an albumin as a drug carrier were also approved, examples are shown in Table 1.[7–16] Furthermore, there are new drugs based on albumin currently in the development and in the clinical trial stages (Table 1).[17–19] For example, Albuferon® (Human Genome Sciences, Rockville, Maryland), a fusion protein of albumin and interferon-α-2b for the treatment of hepatitis C infections, is expected to improve the treatment by allowing a monthly dosing schedule in clinics.[11,20,21]

In addition to drug development in the pharmaceutical industry, there is a growing interest in exploring various pharmaceutical applications of albumin as a drug carrier in academic research. Many researchers have used different approaches to develop novel albumin-based drug carriers and these can be generally categorized into three main modifications: (1) low-molecular-weight proteins fused with albumin,[22,23] (2) polymerization,[24–29] (3) surface modification[30–33] (Fig. 2). The main objectives of these modifications were to prolong blood retention or to enhance the delivery of a drug to the target area, and their effectiveness and usefulness for various

Table 1. Overview of Albumin-based Drugs that have Received Market Approval or are in Clinical Development

	Formation with Albumin	Application	Effect of Albumin
Levemir®	The albumin-binding derivative of human insulin	Type 1 and 2 diabetes	Increment of half-life (native insulin, 4–6 min; Lavemir®, 5–7 h)
Nanocoll® (Nycomed Amersham Sorin, Milan, Italy) Albures® (Sorin Biomedical, Irvine, CA) Pulmolite® (Du Pont Pharma, North Billerica, NA) Draximage® (draxlmage Inc., London, UK)	Tecnetium^{99m} (^{99m}Tc)-aggregated albumin	γ-emitting radionuclide imaging agent	Increment of the accumulation in targeting area
Abraxane®	Albumin–paclitaxel nanoparticle	Solid tumors	Increment of accumulation and uptake in tumor
Albuferon™	Fusion protein of albumin and interferon-α-2b	Hepatitis C infection	Increased blood retention
Vasovist® (Schering AG, Berlin, Germany)	Gadofosveset reversibly binds to human serum albumin	Magnetic resonance contrast agent	Higher relaxivity and extended intravascular enhancement
MARS™ (Gambro, Lund, Sweden)	Dialysis solution containing human serum albumin across a high-flux permeable membrane	Liver failure	Increment of effectively removing albumin-bound endogenous or exogenous toxin

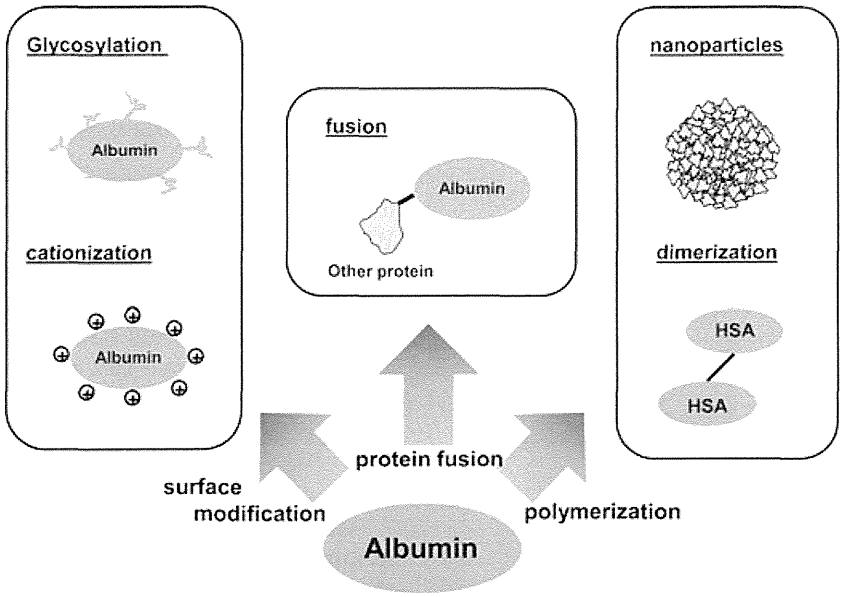

Figure 2. Albumin, a versatile drug carrier for surface modification, small molecular protein fusion, and polymerization.

clinical applications have been demonstrated in many reports. Among these modifications, albumin dimerization has great potential and advantages for clinical applications as both a plasma expander and a drug carrier, whereas other forms of albumin modifications could achieve only one of these two clinical applications. Furthermore, several investigators have clearly shown that increased concentrations of albumin dimers are present in the circulating blood of patients with chronic renal disease as compared with age-matched healthy individuals[34,35] as well as the concentration of products resulting from oxidative damage in the blood.[36,37] These results imply that the albumin dimer also has the potential for use as a biomarker of oxidative stress. Despite multiple applications of albumin dimers, more work will be needed to obtain a better understanding of the biological/physicochemical properties of such preparations. In this review, we summarize the present state of knowledge regarding the albumin dimer to provide justification for the need to obtain further experimental data.

STRUCTURAL CHARACTERISTICS OF ALBUMIN DIMERS

Design

An albumin dimer was first prepared by Straessle and coworkers[38,39] in 1954 as the result of a reaction with mercury (II) or oxidation with iodine, as shown below:

$$\text{Albumin} - \text{S} - \text{Hg} - \text{S} - \text{Albumin} + \text{I}_2$$
$$= \text{Alb} - \text{S} - \text{S} - \text{Alb} + \text{HgCl}_2$$

The HSA dimer produced by direct Cys34–Cys34 disulfide linkage of two HSA molecules has several disadvantages: (1) side reactions with other residues during preparation, (2) low stability, (3) structural disorganization of the albumin dimer that results in decreased ligand binding.[40,41] Therefore, in the past, most researchers did not consider such albumin dimers as ideal candidates for use in clinical applications as a plasma expander and drug carrier.

On the basis of electron spin resonance measurements and a crystal structural analysis of rHSA, the Cys34 thiol is located in a hydrophobic crevice with a depth of 9.5–10 Å.[42–45] This implies that intermolecular Cys34 disulfide bridging might lead to flattening of the pocket. Therefore, linking two rHSA molecules via the use of a flexible spacer to avoid such steric strain is the currently preferred strategy for producing new types of rHSA dimers. Recently, several investigators chemically or genetically produced the next generation of albumin dimers, which are produced using a 10 amino acids spacer via the C and N termini or 1,6-bis(maleimido)hexane (BMH) via the Cys 34 residues.[28,29,46]

Komatsu et al.[28,47] produced an rHSA dimer by linking two rHSA molecules with BMH, which is sufficiently long (16.1 Å) to permit the Cys34 residues on two HSA molecules to be connected without causing much strain on the overall structure of the protein (Fig. 3a). They completely converted the non-mercaptoalbumin to mercaptoalbumin using dithiothreitol, and subsequently established methods of preparation and purification of rHSA dimer via a chemical approach. These established conditions permitted the dimer to be recovered with 99% purity and

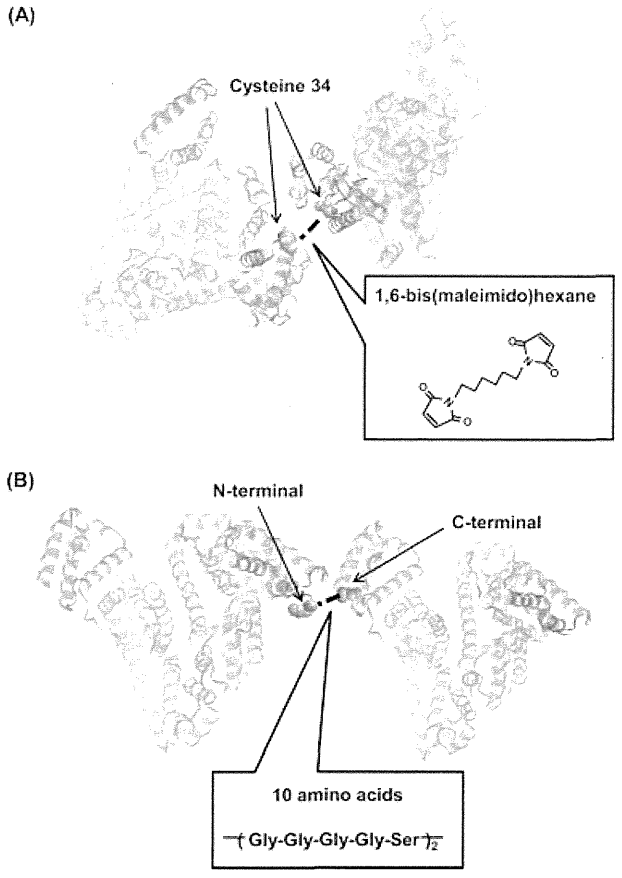

Figure 3. Simulated structure of an rHSA dimer (a) in which the Cys34 residues are cross-linked by reaction with 1,6-bis(maleimido)hexane (BMH) and (b) genetically linked with an amino acid linker $(GGGGS)_2$.

at an 80% yield. In addition, the stability of the purified BMH-bridged rHSA dimer solution (in phosphate buffered saline, 20 g/dL) remained unchanged for a period of over 1 year at room temperature and no aggregation or precipitation was observed during this period of time (Fig. 4a).

Matsushita et al.[29] prepared an rHSA dimer in which two HSA molecules were genetically linked with an amino acid linker $(GGGGS)_2$ (Fig. 3b). A flexible and highly hydrophilic polypeptide linker is generally used for producing fusion proteins.[48–50] They constructed the rHSA dimer expression vector through four-piece ligation. Subsequently, the expression vector of the rHSA dimer was transformed into *Escherichia coli* JM109 and amplified. The resulting vector was linearized with *Sal*I and introduced into the yeast *Pichia pastoris* (strain GS115), which secretes the genetic rHSA dimer. The best expression of the genetic rHSA dimer was also established by regulating the composition, pH, temperature, and methanol concentration of the medium. Finally, the genetic rHSA dimer was purified on gel column chromatography, and subsequently defatted using a charcoal procedure, deionized, freeze dried, and then stored at −20°C (Fig. 4b).

Physicochemical Properties

As previously described (Fig. 4a), the chemical rHSA dimer is linked via Cys34 residues of two rHSA with BMH, whereas the genetic rHSA dimer is linked at the C-terminal of the one rHSA to the N-terminal of another rHSA molecule with a peptide linker comprises 10 amino acids $(GGGGS)_2$. The physicochemical properties of the two rHSA dimers might be different because of structural difference at the site of linkage. In this section, the physicochemical properties of these two rHSA dimers are summarized as follows (Table 2).

An X-ray crystal structure of rHSA dimer is not available at present. The molecular weight of both the chemical and genetic rHSA dimers was approximately twice the molecular weight of the HSA monomer. Furthermore, the secondary and tertiary protein structures, deduced by far-ultraviolet (UV) and near-UV circular dichroism (CD) measurements, clearly showed that a slight decrease in the molar ellipticity of the genetic rHSA dimer had occurred in comparison with that of native HSA in the far-UV CD spectrum, and the near-UV CD spectra of the genetic rHSA dimer show the same minima and shape as that of native HSA. Although it is unclear why there is a difference in the far-UV CD between the HSA monomer (native and rHSA)[51] and the genetic rHSA dimer, it is highly possible that the peptide linker comprises 10 amino acids itself produces a cotton effect that contributes to the overall CD spectra of the genetic rHSA dimer, but the chemical linker does not produce an effect to the same extent as the peptide linker. On the contrary, the far-UV CD spectrum of the BMH-bridged rHSA dimer was identical to that of the rHSA monomer. These results suggest that the structural aspects of both chemical and genetic rHSA units in the dimer are similar to that of the HSA monomer.

Concerning the thermal stability of the rHSA dimer, the BMH-bridged rHSA dimer has a similar exothermic denaturing temperature (T_d) as the rHSA monomer. In addition, only the enthalpy change during the denaturation (ΔH) was slightly lower than twice the monomer's value. On the contrary, the midpoint of the denaturation temperature (T_m) and enthalpy of transition (ΔH_m) of the genetic rHSA dimer were identical to those in the native HSA monomer. In general, plasma HSA is pasteurized at a temperature of 333 K for 10 h to eliminate viral contaminants, for example, hepatitis, HIV, and the herpes virus.[52] The above-mentioned findings indicate that both the chemical and genetic rHSA dimers have the same thermodynamic stability as the rHSA monomer,

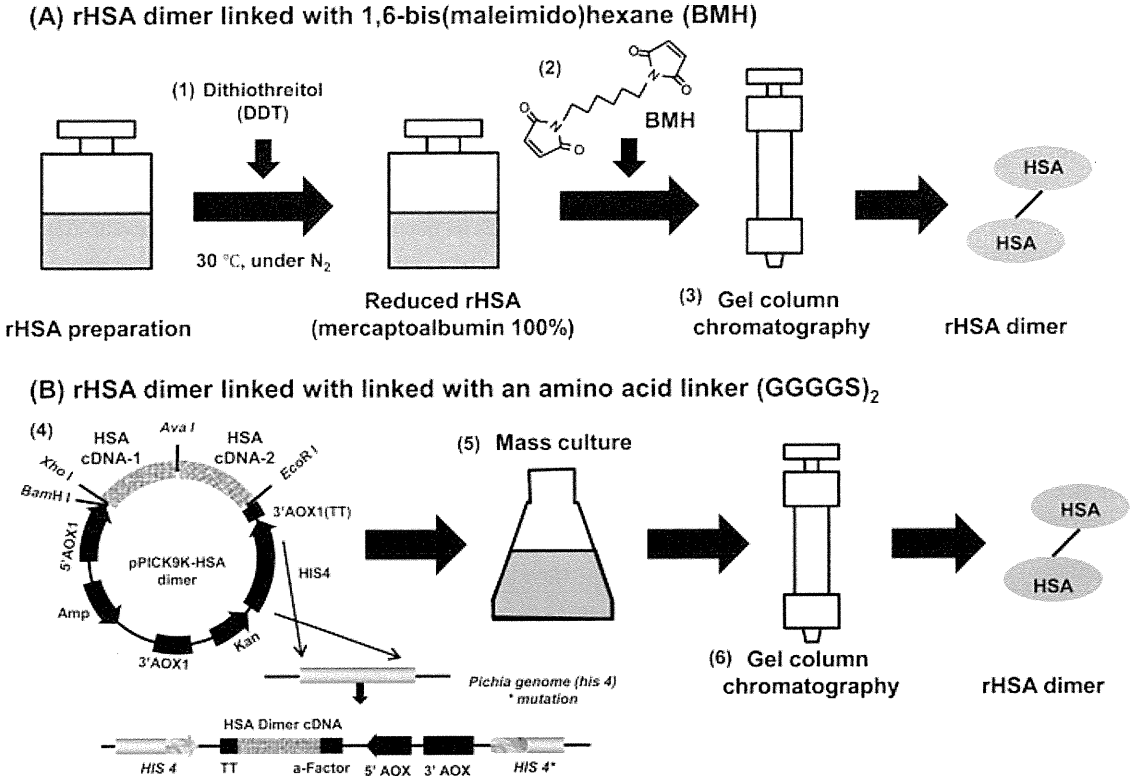

Figure 4. Scheme for the preparation of a (a) recombinant HSA dimer chemically linked with 1,6-bis(maleimido)hexane (BMH) and a (b) rHSA dimer genetically linked with an amino acid linker $(GGGGS)_2$. (1). To reduce the Cys34 in rHSA, dithiothreitol added to the rHSA solution. (2). The ethanolic BMH was added dropwise into the rHSA solution, and was then gently stirred overnight at room temperature. (3). The BMH-bridged rHSA dimer was purified by gel column chromatography. (4). The rHSA dimer expression vector was constructed through the four-piece ligation of the following: (i) the pPIC9K vector was digested with *Bam*HI and *Eco*RI; (ii) the fragment derived from the digestion of pPIC9K with *Bam*HI and *Xho*I restriction sites; (iii) the PCR product on the 50 side of the rHSA dimer digested with *Xho*I and *Ava*I (HSA cDNA-1); (iv) the PCR product on the 30 side of the rHSA dimer digested with *Ava*I and *Eco*RI (HSA cDNA-2). (5). An overnight preculture of the best expression recombinant yeast was used to inoculate of glycerol complex medium for 2 days at 30°C and in a buffered 250 mL methanol complex medium for subsequent 4 days. (6). The secreted genetic rHSA dimer was purified by gel column chromatography.

and therefore heat pasteurization can be used to sterilize the rHSA dimer.

Although HSA accounts for only 60% of the mass of the total plasma proteins, it is responsible for 80% of the colloid osmotic pressure of plasma (25–33 mmHg). Therefore, it is important to determine the colloid osmotic pressure contributed by the rHSA dimer. From the relationship between the protein concentration and the colloid osmotic pressure, the colloid osmotic pressure of the BMH-bridged and genetic rHSA dimer solutions at physiological concentrations (5 g/dL) was approximately 9 mmHg, which is less than half that of the native HSA and rHSA monomer.[28,47] Komatsu et al.[47] analyzed the slope of a plot of the colloid osmotic pressure–protein concentration versus protein concentration that provides the second virial coefficient that accounted for the protein Donnan effect, and the intercept that corresponds to the molecular weight of the protein. The analysis resulted in the expected molecular weights for monomeric and dimeric HSA, which are consistent with the osmotic pressure differences.[47]Thus, physiological colloid osmotic pressure can be maintained using the rHSA dimer at a concentration equivalent to 5 g/dL of the HSA monomer.

BIOLOGICAL PROPERTIES

Compatibility and Immunogenicity

Only a few studies have appeared regarding the biocompatibility of the albumin dimer. As a result of an *in vitro* study, the numbers of blood cells, such as red blood cells (RBCs), white blood cells, and platelets,

Table 2. Comparison of the Structural and Biological Characteristics Among the HSA Monomer, Chemical, and Genetic HSA Dimers

	HSA Monomer	Chemical HSA Dimer46	Genetic HSA Dimer29
MW (Da)	66,331[a,b]	132,741[b]	~130,000[c]
p*I*	4.8[a]	4.8	–
CD			
Near	–	–	Identical to HSA monomer
Far	–	Identical to HSA monomer	Decrease in the molar ellipticity
Thermal stability			
T_m (K)	337.1 ± 0.1[d]	–	341.6 ± 0.6
ΔH_m (kJ/mol)	198.8 ± 4.4[d]	–	197.1 ± 18.8
T_d (K)	336[a]	338	–
COP (mmHg)	18–20[a,d]	9–10	9–10
Ligand binding (M^{-1})			
Site I			
Warfarin	3.8×10^5[a]	3.8×10^5	–
CMPF	$9.8 \pm 3.3 \times 10^5$[d]	–	$8.8 \pm 2.5 \times 10^5$
Site II			
Diazepam	1.4×10^5[a]	1.7×10^5	–
Ketprofen	$3.2 \pm 0.2 \times 10^5$[b]	–	$4.0 \pm 1.3 \times 10^5$
Disposition	–	Longer than HSA monomer	Longer than HSA monomer

Value obtained from recombinant HSA monomer[a] and native HSA monomer[d].
Determined by Matrix Assisted Laser Desorption/Ionization-Time of Fight/Mass Spectrometry (MALDI–TOF/MS)[b] and Sodium dodecyl sulfate-polyacrylamide gel electrophoresis (SDS-PAGE)[c].
MW, molecular weight; p*I*, the isoelectric point; CD, circular dichrosim; T_m, midpoint of denaturation temperature; ΔH_m, enthalpy change during denaturation; T_d, denaturing temperature; COP, colloid osmotic pressure.

after the addition of the rHSA dimer to whole blood were identical to control experiments in which saline or the rHSA monomer were used. Furthermore, several investigators detected the increased presence of the albumin dimer, which comprises two HSA molecules linked via a Cys34–Cys34 disulfide linkage produced by oxidative damage in the blood circulation, in human plasma of patients with chronic renal disease.[35] The albumin dimer has also been detected in the urine of patients with renal impairment, possibly due to a malfunctioning glomerulus.[52–54] This suggests that the albumin dimer is naturally generated and is present in the human body. Therefore, it can be concluded that no specific interactions occurred between the rHSA dimer and blood cell components. On the contrary, Komatsu et al.[47] analyzed the immunological reactivity of the BMH-bridged rHSA dimer using an anti-HSA polyclonal antibody and confirmed that the BMH-bridged rHSA dimer conserves the antigen epitopes of the rHSA monomer and native HSA monomer. No incidence of anaphylaxis or immunological responses were reported following the intravenous administration of both chemical and genetic rHSA dimers under the experimental conditions used, but further *in vitro* and *in vivo* studies will be needed to determine whether the rHSA dimers have the potential to raise any immunological responses.

Pharmacokinetic Properties

Ligand Binding Capacity

Human serum albumin has two major endogenous and exogenous ligand binding sites, namely Site I and Site II.[55,56] Sollenne et al.[41] performed the first study of the ligand binding properties of the HSA dimer. They separated the HSA monomer and the dimer in commercial HSA by gel filtration, and determined the reactivity of the HSA monomer and dimer with *p*-nitrophenyl acetate (NphOAc) and tryptophan. The findings indicated that the HSA dimer reacted with NphOAc 10% as fast as the HSA monomer, and the HSA dimer also showed little affinity for tryptophan. On the basis of structural information on the hydrodynamic and ligand binding sites at that time,[57,58] it was concluded that the absence of a binding site in the dimer might reflect its inclusion within the dimer interface of the direct Cys34–Cys34 disulfide linked HSA dimer.

Komatsu et al.[47] determined the binding constants for warfarin (a Site I ligand) and diazepam (a Site II ligand), for the BMH-bridged rHSA dimer using an ultracentrifugation method. The equilibria are expressed by the following equations:

$$D + L \underset{}{\overset{K_1}{\rightleftharpoons}} D - L$$

$$D - L + L \overset{K_2}{\rightleftharpoons} D - L_2$$

$$D + 2L \overset{K_{apps}}{\rightleftharpoons} D - L_2.$$

where D is the rHSA dimer and L represents the ligand. The binding constant (k) of each ligand was estimated to be 3.0×10^5 and 1.7×10^5 M^{-1}, respectively, which were comparable to that for the rHSA monomer.[47] Furthermore, the binding constants (k) for a Site I ligand [3-carboxy-4-methyl-5-propyl-2-furanpropanic acid (CMPF)] and a Site II ligand